1324 J. Am. Chem. Soc. 1994, 116, 1324–1336

# Reversible Dioxygen Binding and Aromatic Hydroxylation in O$_2$-Reactions with Substituted Xylyl Dinuclear Copper(I) Complexes: Syntheses and Low-Temperature Kinetic/Thermodynamic and Spectroscopic Investigations of a Copper Monooxygenase Model System

**Kenneth D. Karlin,* M. Sarwar Nasir, Brett I. Cohen, Richard W. Cruse,† Susan Kaderli,† and Andreas D. Zuberbühler†**

*Contribution from the Departments of Chemistry, The Johns Hopkins University, Baltimore, Maryland 21218, State University of New York at Albany, Albany, New York 12222, and Institute of Inorganic Chemistry, University of Basel, CH-4056 Basel, Switzerland*

*Received September 16, 1993*[⊗]

**Abstract:** The binding and subsequent reactivity of dioxygen (O$_2$) upon binding to copper ion centers is of fundamental interest in chemical and biological processes. We provide here a detailed account of the reaction of O$_2$ with dicopper(I) complexes, involving O$_2$-reversible binding, followed by the stoichiometric aromatic hydroxylation of the ligand, Thus, tricoordinated dicopper(I) complexes [Cu$_2$(R–XYL)]$^{2+}$ (R = H, MeO, *t*-Bu, F, CN, NO$_2$; **1a–f**) possess dinucleating meta-substituted xylylene ligands with two chelating tridentate bis[2-(2-pyridyl)ethyl]amine (PY2) moieties and a 5-R substituent. Upon reaction with O$_2$, dioxygen adducts [Cu$_2$(R–XYL)(O$_2$)]$^{2+}$ (**2a,c–f**) form reversibly, and these subsequently yield 2-xylylene-hydroxylated products [Cu$_2$(R–XYL–O$^-$)(OH)]$^{2+}$ (**3a–f**), which are phenoxo- and hydroxo-bridged copper(II) complexes. The products **3** have been characterized via the X-ray structure of the parent complex **3a**, and by their UV–visible, infrared, and room-temperature magnetic properties. Incorporation of the O-atom from dioxygen into the phenolic products has been proven by isotopic labeling experiments, except in the case of **3f**, where workup results in an exchange reaction causing loss of the oxygen label. In reactions of O$_2$ with **1** in dichloromethane at room temperature, 10–25% yields of unhydroxylated complexes [Cu$_2$(R–XYL)(OH)]$^{3+}$ (**5**) are obtained. A stopped-flow kinetics study of O$_2$ reactions of **1** in CH$_2$Cl$_2$ demonstrates that [Cu$_2$(R–XYL)(O$_2$)]$^{2+}$ (**2a,c–f**) complexes form reversibly, proceeding via the reaction **1** + O$_2$ ⇄ **2** ($K_1 = k_1/k_{-1}$); this is followed by the irreversible reaction **2** → **3** ($k_2$). Analysis of temperature-dependent data which is accompanied by spectrophotometric monitoring yields both kinetic and thermodynamic parameters for R = H, *t*-Bu, F, and NO$_2$. Dioxygen binding to **1** occurs in a single observable step with low activation enthalpies (6–29 kJ mol$^{-1}$) and large, negative activation entropies (–66 to –167 J K$^{-1}$ mol$^{-1}$). The remote R-substituent has a significant effect on the dioxygen-binding process and this is explained in terms of its multistep nature. Strong binding ($K_1$) occurs at low temperature (e.g. –80 °C), and thermodynamic parameters indicate a large enthalpic contribution ($\Delta H° = -52$ to $-74$ kJ mol$^{-1}$), but room-temperature stabilities of the dioxygen adducts are precluded by very large unfavorable entropies ($\Delta S° = -156$ to $-250$ J K$^{-1}$ mol$^{-1}$). Electron-releasing R-substituents cause a small but significant enhancement of $k_2$, the hydroxylation step, consistent with a mechanism involving electrophilic attack of the Cu$_2$O$_2$ intermediate **2** upon the xylyl aromatic ring. The influence of substituent upon the various rates of reaction allows for stabilization (~minutes), allowing the bench-top observation of **2d,e,f** using UV–visible spectroscopy at –80 °C. "Vacuum-cycling" experiments can be carried out on **1f**/**2f**, i.e., the repetitive oxygenation of **1f** at –80 °C, followed by removal of O$_2$ from **2f** by application of a vacuum. Dicopper(I) complexes **1** have been characterized by $^1$H and $^{13}$C NMR spectroscopy, along with analogs in which an ethyl group has been placed in the 5-position of the pyridyl ring donor groups, i.e., [Cu$^{\text{I}}_2$(R–XYL–(5-Et–PY))]$^{2+}$ (**1g**, R = H; **1h**, R = NO$_2$). Variable-temperature $^1$H NMR spectroscopic studies provide clues as to why [Cu$_2$(MeO–XYL)]$^{2+}$ (**1b**) does not oxygenate (i.e., bind O$_2$ and/or hydroxylate) at low temperature, the conclusion being that significant interactions of the coordinately unsaturated copper(I) ion(s) with the chelated methoxybenzene group result in conformations unsuitable for O$_2$-reactivity. The biological implications of the biomimetic chemistry described here are discussed, as a system effecting oxidative C–H functionalization using O$_2$ under mild conditions and as a monooxygenase model system for tyrosinase (phenol *o*-monooxygenase), with its dinuclear active site.

## Introduction

In the last few years, we have detailed the chemistry of a copper monooxygenase biomimetic system, wherein reaction of dioxygen with a dinuclear copper(I) complex [Cu$_2$(H–XYL)]$^{2+}$ (**1a**) produces a copper–dioxygen Cu$_2$O$_2$ intermediate [Cu$_2$(H–XYL)(O$_2$)]$^{2+}$ (**2a**), which is transformed into a hydroxylated phenoxo and hydroxo doubly bridged dicopper(II) complex [Cu$_2$(H–XYL–O$^-$)(OH)]$^{2+}$ (**3a**) (Figure 1).[1–6] The reaction represents a process

---

[*] To whom correspondence should be addressed at the Department of Chemistry, The Johns Hopkins University, Charles and 34th Streets, Baltimore, MD 21218.

[†] University of Basel.

[⊗] Abstract published in *Advance ACS Abstracts,* January 15, 1994.

(1) Karlin, K. D.; Tyeklár, Z.; Zuberbühler, A. D. In *Bioinorganic Catalysis*; Reedijk, J., Ed.; Marcel Dekker: New York, 1993; pp 261–315.

(2) (a) Karlin, K. D.; Tyeklár, Z. In *Bioinorganic Chemistry of Copper*; Karlin, K. D., Tyeklár, Z., Ed.; Chapman & Hall: New York, 1993; pp 27–291. (b) Tyeklár, Z.; Karlin, K. D. *Acc. Chem. Res.* **1989**, *22*, 241–248.

(3) Karlin, K. D. *Science* **1993**, *261*, 701–708.

(4) (a) Nasir, M. S.; Cohen, B. I.; Karlin, K. D. *J. Am. Chem. Soc.* **1992**, *114*, 2482–2494. (b) Karlin, K. D.; Cohen, B. I.; Jacobson, R. R.; Zubieta, J. *J. Am. Chem. Soc.* **1987**, *109*, 6194–6196.

(5) Cruse, R. W.; Kaderli, S.; Karlin, K. D.; Zuberbühler, A. D. *J. Am. Chem. Soc.* **1988**, *110*, 6882–6883.

(6) Karlin, K. D.; Hayes, J. C.; Gultneh, Y.; Cruse, R. W.; McKown, J. W.; Hutchinson, J. P.; Zubieta, J. *J. Am. Chem. Soc.* **1984**, *106*, 2121–2128.

0002-7863/94/1516-1324$04.50/0

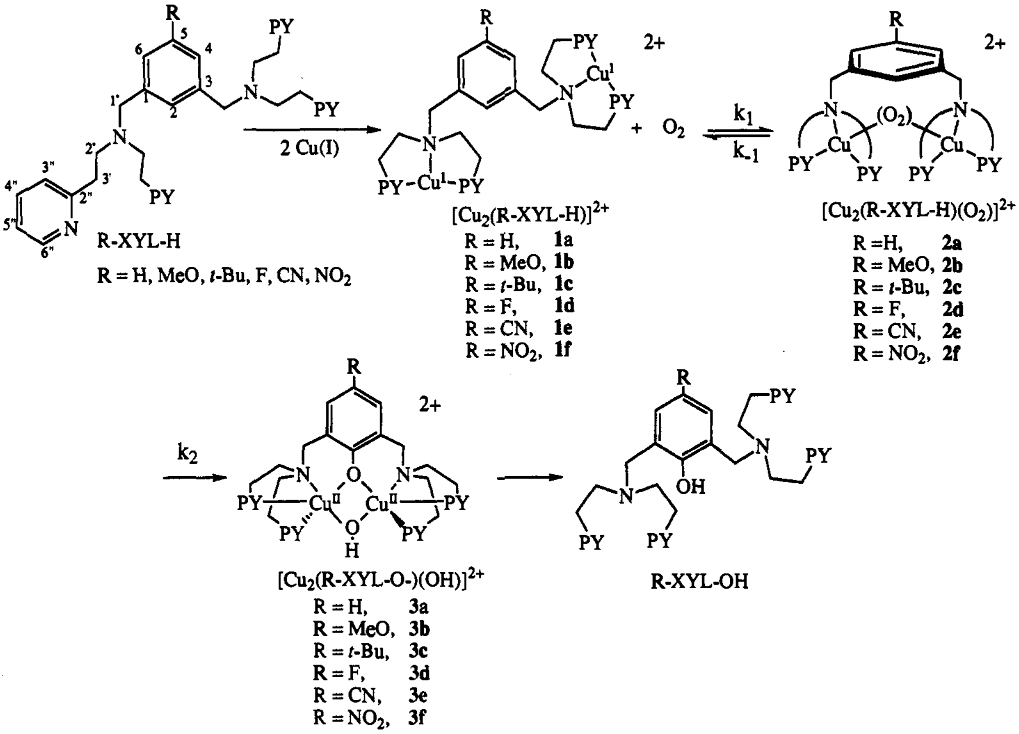

**Figure 1.** Formation of **3a–f**. Ligands R–XYL–H form dicopper(I) complexes **1a–f**, which react with dioxygen reversibly, giving $Cu_2O_2$ adducts **2a–f**, whereupon hydroxylation or the xylyl ligand produces dicopper(II) complexes **3a–f**. Removal of copper ion releases the free phenols R–XYL–OH, completing the copper-mediated hydroxylation of arenes, representing a copper monooxygenase biomimetic system. PY = 2-pyridyl.

involving the activation of dioxygen for hydrocarbon (e.g., aryl) oxygenation, reminiscent of a number of copper proteins,[7–10] especially tyrosinase with its well-established dinuclear copper active site.[7–11] For the parent complex **1a**, we established (i) the stoichiometry of this addition reaction,[6] (ii) that the O-atom in the hydroxylated product **3a** and the XYL–OH ligand was derived from $O_2$,[6] (iii) the kinetic scheme shown, with initial reversible $O_2$-binding ($k_1$ and $k_{-1}$) followed by an irreversible oxygenation step ($k_2$),[5] and (iv) that this latter reaction involves an electrophilic attack of the arene by the $Cu_2O_2$ intermediate **2a**, an example of the "NIH shift" in copper chemistry.[4,12]

The use of various 2-substituted xylyl ligands (i.e., Me, F, D at the site of hydroxylation) was instrumental in obtaining certain mechanistic insights.[1,4a,5] Here, we describe studies involving xylyl ligands with R-substituents OMe, *t*-Bu, F, CN, and $NO_2$ at the 5-position (Figure 1). Dicopper(I) complexes $[Cu_2(R\text{–}XYL)]^{2+}$ (**1b–f**) also hydroxylate to give corresponding products $[Cu_2(R\text{–}XYL\text{–}O^-)(OH)]^{2+}$ (**3b–f**). Characterization of these is provided, along with low-temperature UV–visible studies which give information about dioxygen adduct intermediates $[Cu_2(R\text{–}XYL)(O_2)]^{2+}$ (**2**). Variable-temperature $^1H$ NMR spectroscopic studies provide clues as to why $[Cu_2(MeO\text{–}XYL)]^{2+}$ (**1b**) does not react with $O_2$ at low temperature. Detailed kinetic studies of the oxygenation of **1a–f** are also described, providing considerable insights into (a) the kinetics and thermodynamics for the reversible binding of $O_2$ to dicopper(I) centers and (b) the hydroxylation process **2** → **3**.

## Results and Discussion

**Ligand and Dicopper(I) Complex Synthesis.** The dinucleating ligands were prepared by standard methods (Experimental Section), all proceeding by generation of the 5-substituted *m*-xylene, bromination with *N*-bromosuccinimide to give the $\alpha,\alpha'$-dibromo-*m*-xylene derivative, followed by reaction with the chelating tridentate PY2 (PY2 = bis[2-(2-pyridyl)ethyl]amine). The dinuclear copper(I) complexes were prepared by the addition of 2 equiv of $[Cu^I(CH_3CN)_4]PF_6$ to the solution of appropriate ligand in dichloromethane or acetonitrile under Ar. Perfect C, H, and N combustion analyses were difficult to obtain because nearly all complexes possessed varying amounts of either $CH_3CN$ or $CH_2Cl_2$ solvate (Experimental Section); nevertheless, the purity of the copper(I) complexes was judged to be excellent, as determined by NMR spectroscopy and the constancy of data obtained in the various physical measurements. The complexes are stable under Ar in a variety of polar organic solvents such as dichloromethane, acetonitrile, acetone, or methanol.

**NMR Spectroscopy and Coordination-Induced Shifts.** $^1H$ and $^{13}C$ chemical shift data and assignments[13–16] for the free ligands and their Cu(I) complexes are given in Tables S1 and S2 (supplementary material), respectively. For other purposes,[17,18] XYL ligands which possess a 5-ethyl substituent on the four

---

(7) *Bioinorganic Chemistry of Copper*; Karlin, K. D., Tyeklár, Z., Ed.; Chapman & Hall: New York, 1993.

(8) Solomon, E. I.; Baldwin, M. J.; Lowery, M. D. *Chem. Rev.* **1992**, *92*, 521–542.

(9) Kitajima, N. *Adv. Inorg. Chem.* **1992**, *39*, 1–77.

(10) Sorrell, T. N. *Tetrahedron* **1989**, *45*, 3–68.

(11) (a) Wilcox, D. E.; Porras, A. G.; Hwang, Y. T.; Lerch, K.; Winkler, M. E.; Solomon, E. I. *J. Am. Chem. Soc.* **1985**, *107*, 4015–4027. (b) Robb, D. A. In *Copper Proteins and Copper Enzymes*; Lontie, R., Ed.; CRC: Boca Raton, FL, 1984; Vol. 2, pp 207–241. (c) Lerch, K. *Met. Ions Biol. Syst.* **1981**, *13*, 143–186.

(12) The "NIH shift" involves a 1,2-migration of substituents, observed in the hydroxylation of aromatic substrates for certain iron-containing hydroxylases. See: (a) Guroff, G.; Daly, J. W.; Jerina, D. M.; Renson, J.; Witkop, B.; Udenfriend, S. *Science* **1967**, *158*, 1524. (b) Daly, J.; Guroff, G.; Jerina, D.; Udenfriend, S.; Witkop, B. *Adv. Chem. Ser.* **1968**, *77*, 270. (c) Jerina, D. M. *Chemtech* **1973**, *3*, 120–127.

(13) Pretsch, E.; Clerc, T.; Seibl, J.; Simon, W. *Tables of Spectral Data for Structure Determination of Organic Compounds*; *Chemical Laboratory Practice* (translated from German by R. Biemann); Springer-Verlag: Berlin, 1983.

(14) (a) Crushley, R. J.; Naugler, D.; Ortiz, C. *Can. J. Chem.* **1975**, *53*, 3419. (b) Lavallee, D. K.; Baughman, M. D.; Phillips, M. P. *J. Am. Chem. Soc.* **1977**, *99*, 718–724.

(15) Strothers, J.-B. *Carbon-13 NMR Spectroscopy*; Organic Chemistry Series; Academic: New York, 1972; Vol. 24, pp 29–35.

(16) Kitagawa, S.; Munakata, M.; Miyaji, N. *Inorg. Chem.* **1982**, *21*, 3842–3843.

(17) Nasir, M. S.; Jacobson, R. R.; Zubieta, J.; Karlin, K. D. *Inorg. Chim. Acta* **1993**, *203*, 5–7.

(18) Nasir, M. S. Ph.D. Dissertation, State University of New York (SUNY) at Albany, 1990.

**Table 1.** $^1$H NMR Coordination-Induced Shifts (CIS) for Copper(I) Complexes with Respect to Their Ligands

| complex[a,b] | 6″ | 4″ | 5″,3″ | 4,6 | 2 | 1′ | 2′ + 3′ |
|---|---|---|---|---|---|---|---|
| $[Cu^I_2(H–XYL)]^{2+}$ (**1a**) | +0.05 | +0.30 | +0.20 | +0.15 | | +0.05 | +0.30 |
| $[Cu^I_2(MeO–XYL)]^{2+}$ (**1b**) | –0.10 | +0.20 | +0.20 | –0.45 | +0.20 | 0 | +0.15 |
| $[Cu^I_2(F–XYL)]^{2+}$ (**1d**) | +0.15 | +0.30 | +0.30 | +0.40 | +0.20 | +0.30 | +0.20 |
| $[Cu^I_2(CN–XYL)]^{2+}$ (**1e**) | +0.10 | +0.30 | +0.35 | +0.45 | +0.40 | +0.20 | +0.10 |
| $[Cu^I_2(NO_2–XYL)]^{2+}$ (**1f**) | +0.15 | +0.30 | +0.20 | +0.45 | +0.30 | +0.15 | 0 |
| $[Cu^I_2(H–XYL–(5\text{-Et–PY}))]^{2+}$ (**1g**) | +0.05 | +0.35 | +0.25 | +0.15 | +0.25 | 0 | +0.20 |
| $[Cu^I_2(NO_2–XYL–(5\text{-Et–PY}))]^{2+}$ (**1h**) | +0.20 | +0.35 | +0.35 | +0.20 | +0.30 | +0.05 | +0.20 |

[a] Formation of complex from the respective ligand. [b] Spectra of the complex and its respective ligand were taken in the same solvent.

**Table 2.** UV–Visible, IR, and Magnetic Data for Compounds **3a–f**

| | UV–visible,[a] $\lambda_{max}$, nm ($\epsilon$, $M^{-1}\,cm^{-1}$) | | | IR characteristic peaks | | | magnetic moment,[c] |
|---|---|---|---|---|---|---|---|
| compound | d–d | CT[b] | | OH | | $PF_6$ | $\mu_{eff}$, BM/Cu |
| $[Cu^{II}_2(XYL–O)(OH)](PF_6)_2$ (**3a**) | 635(180) | 440 (sh), 378 (3600) | 330 (2380) | 3605 (br) | | 840 | 0.9 ± 0.1 |
| $[Cu^{II}_2(MeO–XYL–O)(OH)](PF_6)_2$ (**3b**) | 690(300) | 466 (1100) | 390 (sh, 1400) | 3600 (s) | | 840 | 1.1 ± 0.1 |
| $[Cu^{II}_2(t\text{-Bu–XYL–O})(OH)](PF_6)_2$ (**3c**) | 672(160) | 390 (sh, 1800) | 330 (sh, 2210) | 3610 (br) | | 840 | 1.1 ± 0.1 |
| $[Cu^{II}_2(F–XYL–O)(OH)](PF_6)_2\cdot0.5CH_3CN$ (**3d**) | 638(110) | 377 (2200) | | 3640 (s) | | 840 | 1.3 ± 0.1 |
| $[Cu^{II}_2(CN–XYL–O)(OH)](PF_6)_2$ (**3e**) | 685 (210) | 375 (970) | | 3610 (br) | 2240[d] | 840 | |
| $[Cu^{II}_2(NO_2–XYL–O)(OH)](PF_6)_2$ (**3f**) | 689(170) | 345 (11 600) | | 3600 (s) | 1580[e]<br>1380[f] | 840 | 1.5 ± 0.1 |

[a] $CH_3CN$ solution. [b] LMCT. [c] Room temperature. [d] $\nu(CN)$. [e] $\nu_{as}(NO_2)$. [f] $\nu_s(NO_2)$.

pyridyl rings were synthesized. Dicopper(I) complexes of these, i.e., $[Cu^I_2(R\text{-XYL–(5-Et–PY)})]^{2+}$ (**1g**, R = H; **1h**, R = $NO_2$), also react with $O_2$ to give analogous hydroxylated $[Cu^{II}_2(R\text{–XYL–(5-Et–PY)–O}^-)(OH)]^{2+}$ products **3g** (R = H) and **3h** (R = $NO_2$). Since spectra of the ligands and dicopper(I) complexes were important in making NMR assignments, their syntheses are reported in the Experimental Section, and NMR data are also given in Tables S1 and S2.

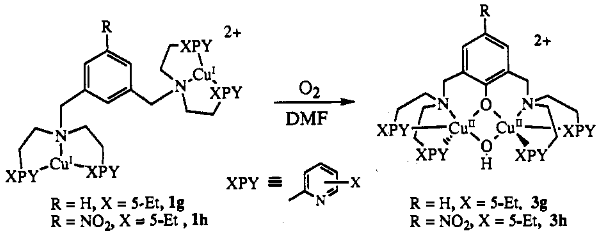

We observe that most free ligand chemical shifts (for hydrogen) move downfield (i.e., positive CIS) upon coordination with copper(I). This is the usual case, due to the deshielding effect of the positively charged metal ion, and these coordination-induced shifts (i.e., CIS's) for **1a,b** and **1d–f** are provided in Table 1. Thus, there is no particular correlation of the CIS with xylyl 5-substituent, as might be expected. The methoxy-substituted complex $[Cu_2(MeO–XYL)]^{2+}$ (**1b**) exhibits somewhat differing behavior, where the phenyl 4 and 6 hydrogen (Figure 1) chemical shifts move *upfield* upon coordination. The benzylic 1′ hydrogens exhibit no shift, while the py-6″ hydrogens move upfield again; for these resonances the effects are less pronounced than those for the 4 and 6 hydrogens. In all other cases, a downfield shift is observed. The rather large effect upon the phenyl hydrogens could be due to (i) $\pi$ interactions between copper and the phenyl ring which may cause an upfield shift due to $\pi$-back donation of electrons from the electron-rich Cu(I) ion to the phenyl ring, i.e., $Cu_\pi \rightarrow \pi^*$ donation, or (ii) a ring current effect induced by pyridine rings coordinated to copper, i.e., due to geometric changes, where pyridine ligand donors come close to the phenyl ring with a methoxy substituent, causing a shielding effect with resultant upfield shifting. We favor the former explanation, in part on the basis of observations from variable-temperature $^1$H NMR spectroscopy and low-temperature oxygenation studies, discussed below.

**Room-Temperature Oxygenation of $[Cu_2(R–XYL)]^{2+}$ (1b–f) in Dimethylformamide (DMF) Giving Hydroxylation Products $[Cu_2(R–XYL–O^-)(OH)]^{2+}$ (3b–f).** As described earlier for $[Cu_2(H–XYL)]^{2+}$ (**1a**),[6] the oxygenation of compounds **1b–f** in DMF at room temperature gives phenoxo and hydroxo bridged dicopper(II) complexes $[Cu_2(R–XYL–O^-)(OH)]^{2+}$ (**3b–f**) (Figure 1). These are isolated in good yield from dark-green (**1c–f**) or purple-brown (**1b**) solutions. The deviating color of $[Cu_2(MeO–XYL–O)(OH)]^{2+}$ (**3b**) is presumably due to an electronic effect of the methoxy substituent. The stoichiometry of these reactions has been established by manometric measurements for uptake of $O_2$ by **1c** and **1f** in DMF at room temperature; Cu/$O_2$ = 2:1, as found for **1a**. After reaction of **1c** with $^{18}O_2$ (99%), field desorption mass spectrometric analysis of *t*-Bu–XYL–OH, isolated by $NH_3$(aq) extraction of the copper ions from product $[Cu_2(t\text{-Bu–XYL–O}^-)(OH)]^{2+}$ (**3c**), showed that the $^{18}O$ label was retained (>90%) (see Experimental Section). This reaffirms the monooxygenase stoichiometry of reaction where the substrate-incorporated oxygen atom is derived from $O_2$. When the analogous experiment with $^{18}O_2$ was run with $[Cu_2(NO_2–XYL)]^{2+}$ (**1f**), field desorption mass spectrometric analysis on the phenol $NO_2$–XYL–OH showed that only $^{16}O$ was incorporated and *no* $^{18}O$ label was found. We suggest that this phenomenon occurs during the reaction workup and is due to an aromatic nucleophilic displacement reaction where the strongly electron withdrawing $NO_2$ substituent facilitates addition of solvent water to the phenolic carbon atom. In fact, copper-mediated nucleophilic aromatic substitution reactions are known[19] and *p*-nitrophenols have been shown to undergo facile phenol oxygen exchange with water.[20]

The doubly bridged copper(II) complexes obtained by oxygenating dicopper(I) complexes $[Cu_2(R–XYL–O^-)(OH)]^{2+}$ (**3b–f**) have been characterized by elemental analysis, IR and UR-visible spectroscopy, and room-temperature magnetic measurements (Table 2). These complexes are presumed to have nearly identical coordination structures, analogous to that of the parent complex $[Cu_2(H–XYL–O^-)(OH)]^{2+}$ (**3a**).[6] Yet, the variations observed in room-temperature magnetic moments and UV–visible spectra reveal that the R-substituent does affect the electronic structures of the complexes, somewhat influencing the magnetic coupling, mediated in part through the phenoxo bridging ligand.[21] All complexes are characterized by a d–d absorption band in the 600–700-nm range. Higher energy absorptions are also observed, and the pattern and band position(s) vary with R-substituent.

---

(19) For example, in the Ullman coupling reaction: Paine, A. J. *J. Am. Chem. Soc.* **1987**, *109*, 1899–1901.

(20) (a) Hengge, A. C. *J. Am. Chem. Soc.* **1992**, *114*, 2747–2748 and references cited therein. (b) Oae, S.; Kiritani, R.; Tagaki, W. *Bull. Chem. Soc. Jpn.* **1966**, *39*, 1961–1967.

(21) Karlin, K. D.; Farooq, A.; Hayes, J. C.; Cohen, B. I.; Rowe, T. M.; Sinn, E.; Zubieta, J. *Inorg. Chem.* **1987**, *26*, 1271–1280.

Recent studies[22] have focused on discussions involving $PhO^- \rightarrow Cu(II)$ and/or $OH^- \rightarrow Cu(II)$ ligand-to-metal charge-transfer (LMCT) origins for these bands seen in the 340–450-nm region, with the exact assignment not being simple. Most often, the $PhO^- \rightarrow Cu(II)$ transitions, which may be of multiple type (e.g., $\sigma$ and $\pi$), usually occur in the 420–470-nm region.[21-25] This charge-transfer band appears to be absent in **3d–f**, and we suggest it is either very weak (as seen in certain other phenoxo-bridged dicopper(II) complexes)[25] or shifted underneath the stronger higher energy CT band(s). The unusually intense 345-nm absorption ($\epsilon$ = 11 600 $M^{-1}\,cm^{-1}$) observed in $[Cu_2(NO_2\text{-}XYL\text{-}O^-)(OH)]^{2+}$ (**3f**) is probably a combination of an $OH^- \rightarrow Cu(II)$ LMCT transition and $NO_2$-perturbed $\pi$–$\pi^*$ absorptions. Hydroxide-to-Cu(II) transitions most likely at least in part involve the higher energy 340–390 absorptions, since these disappear or shift upon substitution of the $OH^-$ ligand by another bridging ligand such as $Cl^-$ or $Br^-$ in **3a**.[21] Observations made in the present complexes **3a–f** thus further indicate that $OR^- \rightarrow Cu(II)$ LMCT transitions are quite sensitive to ligand environment and the electron density at the copper atom.

**Reactivity of $[Cu_2(R\text{-}XYL)]^{2+}$ (1b–f) with $O_2$ in $CH_2Cl_2$.** Oxygenation of these compounds in dichloromethane as a solvent at room temperature usually results in the isolation of two reaction products. The major product is the same hydroxylated dicopper(II) compound $[Cu_2(R\text{-}XYL\text{-}O^-(OH))]^{2+}$ (**3a–f**), as discussed above. Another product is obtained in a yield ranging from 10 to 25%, depending upon the concentration of copper(I) complexes used in the reaction solution. This comes out as a $CH_2Cl_2$-insoluble precipitate, and it is purified by filtration and crystallization from $CH_3CN$/ether. As a minor product during the hydroxylation reaction, it was characterized only in three cases. During the oxygenation of compounds **1c** and **1f** in $CH_2Cl_2$ at room temperature, blue precipitates were formed, whereas in the case of compound **1b**, a green product precipitated. We suggest these unhydroxylated products to be tricationic complexes $[Cu_2(R\text{-}XYL)(OH)]^{3+}$ (**5**) with a single hydroxide bridge formed between the two copper ions coordinated to the ligands. Dichloromethane solvent would seem to be the most likely source of the hydroxide proton. The proposed formulation of these is consistent with physical data (see Experimental Section), including observations that these are EPR silent, in accord with the presence of a bridging $OH^-$ group. No distinct absorptions are present in the 300–600-nm region, consistent with the absence of a phenoxo bridging ligand. Analysis of the dinucleating ligand (obtained by extraction) in these complexes indicates no change from the original, i.e., the benzene ring has not been hydroxylated.

The formation of these unhydroxylated oxidation products $[Cu_2(R\text{-}XYL)(OH)]^{3+}$ (**5**) could be explained by competition for *inter*- rather than *intra*molecular $O_2$-binding processes when $[Cu_2(R\text{-}XYL)]^{2+}$ (**1**) complexes react with $O_2$, apparently favored in dichloromethane solvent compared to dimethylformamide. When carrying out low-temperature UV–visible spectroscopic experiments at relatively low concentrations, i.e., $<10^{-3}$ M, the tricationic $CH_2Cl_2$-insoluble products are never observed, since *intra*molecular $Cu\text{–}(O_2)\text{–}Cu$ formation would be favored. However, at higher concentrations of the dicopper(I) complex **1**, direct reduction of **2** by another molecule of **1** might be favored, the net result being the irreversible four-electron reduction of $O_2$ ($Cu/O_2$ = 4:1) and formation of the tricationic hydroxo complex observed. Another possibility is that higher concentrations of **1** in $CH_2Cl_2$ lead to a cluster species (**4**) incapable of arene hydroxylation, perhaps because the geometry for xylyl attack by the peroxo group is unfavorable.

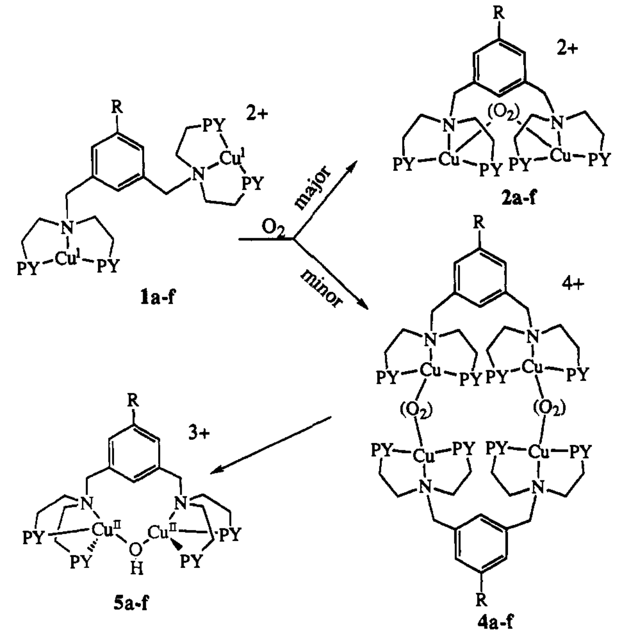

**Low-Temperature Oxygenation Reactions: Kinetics/Thermodynamics of $O_2$-Reactions with $[Cu_2(R\text{-}XYL\text{-}H)]^{2+}$ (1b–f).** In our initially reported study using $[Cu_2(H\text{-}XYL\text{-}H)]^{2+}$ (**1a**),[5] we determined the first complete set of rate constants and activation parameters for reversible dioxygen binding in a copper complexes system, fitting the scheme outlined in Figure 1, i.e., a reversible ($k_1/k_{-1}$) formation of a dioxygen adduct $[Cu_2(H\text{-}XYL\text{-}H)(O_2)]^{2+}$ (**2a**), followed by the irreversible ($k_2$) hydroxylation to give $[Cu_2(H\text{-}XYL\text{-}O^-)(OH)]^{2+}$ (**3a**). The spectroscopic observation of the intermediate $[Cu_2(H\text{-}XYL\text{-}H)(O_2)]^{2+}$ (**2a**) was aided by the favorable relative rates of formation of **2a** and its decomposition to **3a**, i.e., $k_1[O_2] > k_2$, e.g., $k_1$ = 533 $M^{-1}\,s^{-1}$, $k_2$ = 0.0028 $s^{-1}$, and $[O_2] = 2 \times 10^{-3}$ at −80 °C.[5] The study also showed that the copper–dioxygen complex **2a** was thermodynamically stable, with $K_{eq} = 2.7 \times 10^6\ M^{-1}$ (−80 °C), $\Delta H^\circ = -62 \pm 1$ kJ mol$^{-1}$, and $\Delta S^\circ = -200 \pm 6$ J K$^{-1}$ mol$^{-1}$ {Note: the updated final value calculated is $\Delta S^\circ = -196 \pm 6$ J K$^{-1}$ mol$^{-1}$, cf. Table 4}.

In the meantime, the UV–visible properties of $[Cu_2(H\text{-}XYL\text{-}H)(O_2)]^{2+}$ (**2a**) have been shown to closely match those of dinuclear complexes $[Cu_2(Nn)(O_2)]^{2+}$ where Nn is a dinucleating ligand similar to XYL, but having a variable methylene $-(CH_2)_n-$ chain connecting the two PY2 tridentates.[1,2,26] Additionally, extensive spectroscopic and reactivity studies[27] have indicated that the peroxo moieties in $[Cu_2(Nn)(O_2)]^{2+}$ and $[Cu_2(XYL\text{-}Me)]^{2+}$ (for which oxygenation produced a hydroxylation-induced methyl migration, i.e., an "NIH shift"), and thus **2a**, behave as electrophiles and most likely have the bent $\mu$-$\eta^2$:$\eta^2$ side-on structure now known to be found (as a planar $Cu_2O_2$ form) in oxyhemocyanin ($O_2$-carrier)[28] and probably tyrosinase.[8] The lack of a deuterium isotope effect in the reaction of $[Cu_2(H\text{-}XYL\text{-}D)]^{2+}$ (**1a–*D***)[5] is also consistent with a peroxo group in **2a** which attacks the arene xylyl substrate $\pi$-system, as an electrophile.

---

[22] Ling, J.; Farooq, A.; Karlin, K. D.; Loehr, T. M.; Sanders-Loehr, J. *Inorg. Chem.* **1992**, *31*, 2552–2556.

[23] Solomon, E. I.; Penfield, K. W.; Wilcox, D. E. *Struct. Bonding (Berlin)* **1983**, *53*, 1–57.

[24] Amundsen, A. R.; Whelan, J.; Bosnich, B. *J. Am. Chem. Soc.* **1977**, *99*, 6730.

[25] (a) Sorrell, T. N.; O'Connor, C. J.; Anderson, O. P.; Reibenspies, J. H. *J. Am. Chem. Soc.* **1985**, *107*, 4199–4206. (b) Maloney, J. J.; Glogowski, M.; Rohrbach, D. F.; Urbach, F. L. *Inorg. Chim. Acta* **1987**, *127*, L33–L35. (c) Yamauchi, O.; Tsujide, K.; Odani, A. *J. Am. Chem. Soc.* **1985**, *107*, 659–666.

[26] (a) Karlin, K. D.; Tyeklár, Z.; Farooq, A.; Haka, M. S.; Ghosh, P.; Cruse, R. W.; Gultneh, Y.; Hayes, J. C.; Zubieta, J. *Inorg. Chem.* **1992**, *31*, 1436–1451. (b) Karlin, K. D.; Haka, M. S.; Cruse, R. W.; Meyer, G. J.; Farooq, A.; Gultneh, Y.; Hayes, J. C.; Zubieta, J. *J. Am. Chem. Soc.* **1988**, *110*, 1196–1207.

[27] Paul, P. P.; Tyeklár, Z.; Jacobson, R. R.; Karlin, K. D. *J. Am. Chem. Soc.* **1991**, *113*, 5322–5332.

[28] (a) Magnus, K. A.; Ton-That, H.; Carpenter, J. E. In ref 7, pp 143–150. (b) Hazes, B.; Magnus, K. A.; Bonaventura, C.; Bonaventura, J.; Dauter, Z.; Kalk, K.; Hol, W. G. J. *Protein Sci.* **1993**, *2*, 597–619.

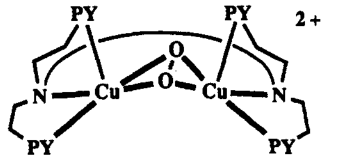

Proposed μ-$\eta^2$:$\eta^2$-Peroxo Dicopper(II) Structure in $[Cu_2(XYL{-}H)(O_2)]^{2+}$ and $[Cu_2(Nn)(O_2)]^{2+}$

Thus, in extending the kinetic/thermodynamic studies to the other R-substituted xylyl complexes, we wished to provide additional insight into the reversible dioxygen binding and the xylyl ring hydroxylation. On the basis of the identical copper-binding sites in all ligands, we assumed that the kinetics and thermodynamics of $O_2$ binding (eq ±1) might be largely unaffected by the variable R-substituent. We also hoped to provide further corroboration of the electrophilic mechanism proposed; we expected that the xylyl ring hydroxylation (eq 2) would be strongly influenced by electronic effects of R = OMe, *t*-Bu, F, CN, and $NO_2$ in the para-position, which should be sterically noninterfering. However, both these expectations turn out to be only partially correct.

$$\underset{\mathbf{1}}{[Cu_2(R{-}XYL)]^{2+}} + O_2 \underset{k_{-1}}{\overset{k_1}{\rightleftharpoons}} \underset{\mathbf{2}}{[Cu_2(R{-}XYL)(O_2)]^{2+}} \qquad (\text{eq } \pm 1)$$

$$\underset{\mathbf{2}}{[Cu_2(R{-}XYL)(O_2)]^{2+}} \xrightarrow{k_2} \underset{\mathbf{3}}{[Cu_2(R{-}XYL{-}O^-)(OH)]^{2+}} \qquad (\text{eq } 2)$$

The reactions of the para-substituted complexes $[Cu_2(R{-}XYL{-}H)]^{2+}$ (**1b–f**) with $O_2$ in dichloromethane were studied using a diode array stopped-flow spectrometer between −100 °C and room temperature. As before,[5] the appearance and then decay of a ~435-nm absorption ascribable to $[Cu_2(R{-}XYL{-}H)(O_2)]^{2+}$ (**2**) was followed; the formation of **2** was complete below −50 °C, $k_{-1}$ being irrelevant. Data collected were reduced by factor analysis and can all be accounted for by the simple two-step mechanism shown in Figure 1 and eqs 1 and 2; no other intermediates are observed. Evolution and subsequent decay of the intermediate peroxo complex are shown for the nitro derivative $[Cu_2(NO_2{-}XYL{-}H)]^{2+}$ (**1f**) in Figure 2, the insert documenting perfect correlation between experimental data and the suggested mechanism. For the hydroxylation step, $k_2$ is composed of a thermal and of a photochemical temperature-independent term, and the latter dominates below ~ −50 °C. It could be accounted for and subtracted out in all cases except that of the $O_2$-reaction with cyano derivative $[Cu_2(CN{-}XYL{-}H)]^{2+}$ (**1e**), where it dominated. This heavy superposition of photochemistry precluded a reasonable kinetics analysis of **1e**. For the temperature-dependent reactions of interest, plots of the kinetic and thermodynamic parameters $\log(k/T)$ or $\log(K_{eq}/T)$ versus $1/T$ are well behaved. Eyring plots for $k_1$, $k_{-1}$, and $k_2$ are shown in Figure 3, again for the nitro derivative **1f**. At the lowest temperatures (−90 to −50 °C), values of $k_1$ only could be used for the calculation of the activation parameters. Rate constants for hydroxylation ($k_2$) would be obscured by the concomitant photoreaction, as already discussed for **1a**,[5] and $k_{-1}$ is irrelevant below −45 °C. Plots corresponding to Figures 2 and 3 were provided for **1a**[5] and are available here as supplementary material for complexes **1c** and **1d**. From the temperature-dependent data, activation parameters for all three rate constants have been deduced; these data and repesentative calculated $k$ values are compiled in Table 3, together with their standard errors as obtained from the regression analyses.

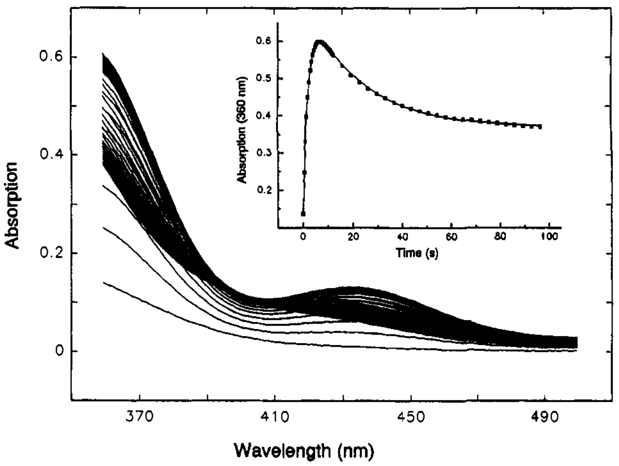

**Figure 2.** Spectral evolution and decay of peroxo complex $[Cu_2(NO_2{-}XYL)(O_2)]^{2+}$ (**2f**) at −60 °C: $[O_2] = 1.9 \times 10^{-3}$ M; $[Cu_2(NO_2{-}XYL)]^{2+} = 1.76 \times 10^{-4}$ M. Insert: Absorbance vs time at 360 nm; (■) experimental data; (—) calculated curve, based on model described by eqs ±1 and 2.

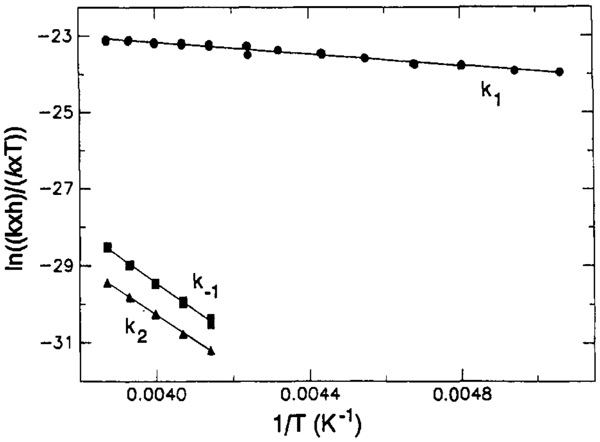

**Figure 3.** Eyring plots for $k_1$, $k_{-1}$, and $k_2$ (eqs ±1 and 2) for $[Cu_2(NO_2{-}XYL)]^{2+}$ (**1f**): $k$, Boltzmann constant, h, Planck constant; $k_1$, pseudo-first-order rate constant including $[O_2] = 1.9 \times 10^{-3}$ M.

In addition to the R = CN complex **1e**, the reaction of $[Cu_2(MeO{-}XYL{-}H)]^{2+}$ with $O_2$ could also not be studied by stopped-flow kinetics. The methoxy complex neither gives a dioxygen adduct nor hydroxylates at low temperature, in spite of the fact that it was expected to undergo the fastest oxygenation reaction on the basis of electronic considerations, since an electrophilic attack by the $Cu_2O_2$ peroxo group is postulated (*vide supra* and ref 4). We assume that hindered rotation of the copper-binding tridentate chelate arms provides the logical explanation, as based on low-temperature NMR studies, discussed below.

**Reversible $O_2$-Binding to $[Cu_2(R{-}XYL{-}H)]^{2+}$ (1).** As can be seen from the data in Table 3, the rapid low-temperature reaction with $O_2$ is characterized by a low activation enthalpy and a large negative activation entropy for all compounds. Such tendencies might be expected on the basis of having reactive, easily oxidizable and coordinately unsaturated (i.e., three-coordinate) cuprous species. An additional important reason for the apparent low-activation enthalpies may be given by the composite nature of the forward reaction (eq +1), *vide supra*: It is hardly conceivable that $O_2$ would bind simultaneously to both copper centers. Rather, we must postulate that $O_2$ first binds to one copper moiety in a rapid, left-lying equilibrium and only in a second step forms the spectroscopically detectable μ-peroxo complex. As these steps themselves are likely to involve significant conformational changes, it seems futile to attribute definitely the values of the activation parameters to any single factor. Nevertheless, the present observations are phenomenologically well in line with previous results for mononuclear complexes possessing tripodal tetradentate

---

(29) (a) Karlin, K. D.; Wei, N.; Jung, B.; Kaderli, S.; Niklaus, P.; Zuberbühler, A. D. *J. Am. Chem. Soc.* **1993**, *115*, 9506–9514. (b) Karlin, K. D.; Wei, N.; Jung, B.; Kaderli, S.; Zuberbühler, A. D. *J. Am. Chem. Soc.* **1991**, *113*, 5868–5870.

**Table 3.** Kinetics Parameters[a] for $O_2$-Interaction with Dicopper(I) Complexes $[Cu_2(R\text{–}XYL\text{–}H)]^{2+}$ (**1a**, **1c**, **1d**, and **1f**)

| | | R | | | |
|---|---|---|---|---|---|
| | | H (**1a**) | *t*-Bu (**1c**) | F (**1d**) | $NO_2$ (**1f**) |
| $k_1$ ($M^{-1}\,s^{-1}$) | 183 K | 385 ± 5 | $(4.9 \pm 0.2) \times 10^2$ | 9.3 ± 0.3 | 109 ± 2 |
| | 223 K | $(1.24 \pm 0.01) \times 10^3$ | $(1.76 \pm 0.03) \times 10^3$ | 331 ± 4 | 281 ± 2 |
| | 298 K | $(5.1 \pm 0.1) \times 10^3$ | $(8.1 \pm 0.4) \times 10^3$ | $(2.2 \pm 0.1) \times 10^4$ | 890 ± 20 |
| | $\Delta H^{\ddagger}$ (kJ $mol^{-1}$) | 8.2 ± 0.1 | 9.1 ± 0.3 | 29 ± 1 | 6.4 ± 0.1 |
| | $\Delta S^{\ddagger}$ (J $K^{-1}\,mol^{-1}$) | −146 ± 1 | −140 ± 1 | −66 ± 1 | −167 ± 1 |
| $k_{-1}$ ($s^{-1}$) | 183 K[b] | $(1.5 \pm 0.4) \times 10^{-5}$ | $(5 \pm 2) \times 10^{-6}$ | $(3 \pm 1) \times 10^{-6}$ | $(1.8 \pm 0.2) \times 10^{-5}$ |
| | 223 K | 0.072 ± 0.005 | 0.11 ± 0.01 | $(4.8 \pm 0.4) \times 10^{-2}$ | 0.024 ± 0.001 |
| | 298 K | $(1.3 \pm 0.2) \times 10^3$ | $(1.2 \pm 0.4) \times 10^4$ | $(4 \pm 1) \times 10^3$ | 99 ± 5 |
| | $\Delta H^{\ddagger}$ (kJ $mol^{-1}$) | 70 ± 1 | 83 ± 4 | 81 ± 3 | 59 ± 1 |
| | $\Delta S^{\ddagger}$ (J $K^{-1}\,mol^{-1}$) | 50 ± 6 | 110 ± 20 | 90 ± 10 | −8 ± 4 |
| $k_2$ ($s^{-1}$) | 183 K | $(3.4 \pm 0.2) \times 10^{-4}$ | 0.007 ± 0.001 | $(1.6 \pm 0.3) \times 10^{-3}$ | $(1.7 \pm 0.1) \times 10^{-5}$ |
| | 223 K | 0.149 ± 0.003 | 1.07 ± 0.04 | 0.188 ± 0.008 | 0.0134 ± 0.0002 |
| | 298 K | 172 ± 8 | 360 ± 40 | 50 ± 8 | 31 ± 1 |
| | $\Delta H^{\ddagger}$ (kJ $mol^{-1}$) | 50 ± 1 | 41 ± 2 | 39 ± 1 | 55 ± 1 |
| | $\Delta S^{\ddagger}$ (J $K^{-1}\,mol^{-1}$) | −35 ± 2 | −59 ± 8 | −82 ± 6 | −32 ± 2 |

[a] All parameters were calculated individually from the appropriate Eyring plots and subsequently rounded off. [b] Relatively uncertain extrapolated values.

**Table 4.** Equilibrium Parameters for $O_2$-Interaction with Dicopper(I) Complexes $[Cu_2(R\text{–}XYL\text{–}H)]^{2+}$ (**1a**, **1c**, **1d**, and **1f**)

| | | R | | | |
|---|---|---|---|---|---|
| | | H (**1a**) | *t*-Bu (**1c**) | F (–1d) | $NO_2$ (**1f**) |
| $K_1$[a] ($M^{-1}$) ($=k_1/k_{-1}$) | 183 K | $2.6 \times 10^7$ | $9.6 \times 10^7$ | $3.3 \times 10^6$ | $5.9 \times 10^6$ |
| | 223 K | $1.7 \times 10^4$ | $1.6 \times 10^4$ | $6.9 \times 10^3$ | $1.2 \times 10^4$ |
| | 298 K | 3.9 | 0.7 | 5.8 | 9.0 |
| | $\Delta H^{\circ}$ (kJ $mol^{-1}$) | −62 ± 1 | −74 ± 4 | −52 ± 3 | −53 ± 1 |
| | $\Delta S^{\circ}$ (J $K^{-1}\,mol^{-1}$) | −196 ± 6 | −250 ± 20 | −156 ± 10 | −159 ± 4 |

[a] Minor inconsistencies with Table 3 are due to rounding errors.

(pyridylalkyl)amino ligands,[29] where substantial activation enthalpies around 30 kJ $mol^{-1}$ were detected for the primary 1:1 $Cu\text{–}O_2$ binding but very small, in fact even negative, ones were observed for the overall formation of the $\mu$-peroxodicopper(II) final product. Among the four derivatives studied, there is a tendency toward compensation with higher enthalpies of activation coupled with more favorable activation entropies and vice versa. The net result is very similar rate constant $k_1$ at the intermediate temperature of 223 K. The activation enthalpies are generally below 10 kJ $mol^{-1}$, and the higher $\Delta H^{\ddagger}$ observed for the fluoro derivative may be related to the hindered rotation mentioned for the R = OMe derivative. Negative $\Delta S^{\ddagger}$ values are consistent with a more highly ordered transition state for partial dioxygen binding.

Trends observed in $\Delta H^{\ddagger}$ for the release of $O_2$ from the $Cu_2O_2$ complex (i.e., $k_{-1}$) suggest that electron-donating groups on the xylyl ring increase the copper–dioxygen bonding strength in $[Cu_2(R\text{–}XYL\text{–}H)(O_2)]^{2+}$ (**2**), and it seems as if the xylyl ring electronic structure had a direct influence on the dioxygen binding, although this would not be primarily expected on the basis of coordination chemical considerations. As for $k_1$, we have a marked compensation again with $k_{-1}$, leading to identical rate constants (i.e., within a factor of 4) at 223 K (Table 3).

From $k_1$ and $k_{-1}$, equilibrium constants $K_1 = k_1/k_{-1}$ and the corresponding thermodynamic parameters $\Delta H^{\circ}$ and $\Delta S^{\circ}$ can be calculated, and they are collected in Table 4. Here again, the $O_2$-binding strength ($\Delta H^{\circ}$) appears to correlate directly with xylyl substituent (R) inductive effects. All of the systems are characterized by large negative standard enthalpies and entropies. As is generally seen in $O_2$-binding by metal complexes,[30–32] increasingly favorable (negative) enthalpies are compensated by larger negative entropies.

As stated above, one would expect the $O_2$-binding properties of $[Cu_2(R\text{–}XYL\text{–}H)]^{2+}$ (**1**) to be rather independent of R and this is supported by the observation that copper ion redox potentials are nearly identical with R = H and R = $NO_2$.[18] The experimental results are somewhat at variance with these expectations (*vide supra*), and the effects are as big or bigger for $O_2$-displacement (i.e., $k_{-1}$) than for ring oxygenation (i.e., $k_2$, *vide infra*). We believe that the dicopper-bound electrophilic peroxo group in $[Cu_2(R\text{–}XYL\text{–}H)(O_2)]^{2+}$ (**2**) (as a $\mu\text{-}\eta^2{:}\eta^2\text{-}O_2^{2-}$ group) is in very close proximity to the xylyl $\pi$-system, and this could provide an exaplanation for the R-group influence upon $O_2$-binding and release. However, a more likely explanation lies in the nature of the $O_2$-binding process as described by $k_1$ and $k_{-1}$, which are in fact composite of at least three steps: (a) preparation of a conformation of **1** suitable for binding $O_2$ to one copper ion, (b) binding of $O_2$ to one copper (intermediate), and (c) formation of the observable peroxide complex **2**. Experimentally, we know that the intermediate cannot be observed under any conditions. It is thus quite unstable, and we have to assume that the transition state for the $O_2$-binding reaction is rather close (i.e., early) to the nonbonded form. Therefore, the observed trends for $k_{-1}$, for example, do *not* reflect actual $O_2$-binding strength in $[Cu_2(R\text{–}XYL\text{–}H)(O_2)]^{2+}$ (**2**) but differences of conformational stabilities in the precursor $[Cu_2(R\text{–}XYL\text{–}H)]^{2+}$ (**1**).

In summary, the thermodynamic data clearly indicate that the quasireversible dioxygen binding is entirely driven by enthalpy, with room-temperature instability due to the large negative entropies. Xylyl group substituents affect the $O_2$-binding strength in a way that suggests some interaction with the aryl ring. The compensating effects seen in $\Delta H^{\circ}$ and $\Delta S^{\circ}$ values lead to rather similar equilibrium constants for $O_2$-binding to complexes $[Cu_2(R\text{–}XYL\text{–}H)]^{2+}$ (**1**), and in fact the relative order of $K_1$ values may be actually reversed by a simple change in temperature. This typical example further serves to caution against deriving conclusions concerning relative stabilities or reactivities on the basis of data obtained at a single temperature.

**Arene Hydroxylation Step, $k_2$.** The kinetics as well as the stereoselectivities in the formation of products preclude that a Fenton-type mechanism (production of hydroxyl radical) is involved in the reaction, e.g., that an intermediate peroxo species is further attacked by LCu(I). We also note that [Cu₂(H-XYL–

---

(30) Niederhoffer, E. C.; Timmons, J. H.; Martell, A. E. *Chem. Rev.* **1984**, *84*, 137–203.

(31) Jones, R. D.; Summerville, D. A.; Basolo, F. *Chem. Rev.* **1979**, *79*, 139–179.

(32) Fallab, S.; Mitchell, P. R. *Adv. Inorg. Bioinorg. Mech.* **1984**, *3*, 311–377.

**Table 5.** UV–Visible Spectral Properties of Metastable Dioxygen Complexes **2d–f** ($CH_2Cl_2$, –80 °C)

| dioxygen complex | molarity | $\lambda_{max}$, nm ($\epsilon$, $M^{-1}$ $cm^{-1}$) | | | stability |
|---|---|---|---|---|---|
| $[Cu_2(t\text{-Bu–XYL})(O_2)]^{2+}$ (**2c**) | $8.0 \times 10^{-5}$ | 362 (16000) | 440 (4000) | 530[a] (1000) | {from kinetics only} |
| $[Cu_2(\text{F–XYL})(O_2)]^{2+}$ (**2d**) | $1.1 \times 10^{-4}$ | 360 (11000) | 436 (2600) | 530 (1000) | ~15–20 min |
| $[Cu_2(\text{CN-XYL})(O_2)]^{2+}$ (**2e**) | $1.0 \times 10^{-4}$ | 358 (16000) | 435 (4000) | 530[a] (1000) | ~40–50 min |
| $[Cu_2(NO_2\text{–XYL})(O_2)]^{2+}$ (**2f**) | $4.9 \times 10^{-5}$ | 358 (20000) | 435 (5000) | 530[a] (1200) | >1 h |

[a] Shoulder.

$H)]^{4+}$ cleanly meets with $H_2O_2$ to give product $[Cu_2(\text{H–XYL–O}^-)(OH)]^{2+}$ (**3a**),[33] while reaction of $[Cu_2(\text{H–XYL–H})]^{2+}$ (**1a**) with hydrogen peroxide does not.[34] Addition of radical traps to solutions of **1** and $O_2$ also does not affect the hydroxylation.[34] The consistent picture for this arene hydroxylation is an electrophilic attack of the bound peroxo ligand, in accord with (1) the lack of a deuterium isotope effect for $[Cu_2(\text{H–XYL–}D)]^{2+}$ (**1a**-*D*),[5] (2) the NIH shift behavior,[4] and (3) the electrophile behavior of the peroxo group in $[Cu_2(Nn)(O_2)]^{2+}$,[27] *vide supra*.

The kinetic data (i.e., for $k_2$, Table 3) are basically in accord with these notions. There is an increase in $\Delta H^{\ddagger}$ with the electron-withdrawing power of R. The compensating effect of activation entropies $\Delta S^{\ddagger}$ makes linear free energy relationship analysis based on plots of log $k_2$ versus $\sigma_p^+$ problematic. Nevertheless, $k_2$ decreases with electron-withdrawing character of R in the whole temperature range studied and, e.g., at –80 °C a very modest $\rho$ of ~ –2.1 is obtained. There are two main possibilities to explain the relatively weak substituent effect: (1) $k_2$ is a composite rate constant, reflecting what must be multiple steps occurring between formation of $[Cu_2(\text{R–XYL–H})(O_2)]^{2+}$ (**2**) and production of $[Cu_2(\text{R–XYL–O}^-)(OH)]^{2+}$ (**3**). Thus, the peroxo ligand attacks the arene, forming a O–C bond and giving a carbocation intermediate, and there must be C–H cleavage and loss of $H^+$ upon rearomatization or methyl 1,2-migration if the initial complex possesses a 2-methyl substituent; these steps are part of the NIH shift discussed in detail elsewhere.[1,4] In addition, O–O cleavage must occur, leading to Cu–O–Cu or Cu–OH–Cu products.[1,4] (2) The peroxo group in **2** may be so reactive an electrophile that it is not sensitive to arene electronic changes in its attack of the xylyl ring. While the reactivity of the peroxo group is clearly seen to be that of an electrophile, we don't see it as being an intrinsically powerful one, and a more likely explanation for its reactivity and relative insensitivity to substituent would be the peroxo group's ideal positioning for p–π attack along the O–O vector.[1,4] A stick molecular model supports this notion, in terms of the facile formation of the structure depicted below.

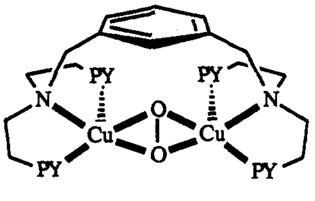

**Bench-Top Reactivity of $[Cu_2(\text{R–XYL})]^{2+}$ (1b–f) with $O_2$ in $CH_2Cl_2$ at Low Temperature.** When a "bench-top" low-temperature (–80 °C) oxygenation of $[Cu_2(\text{H–XYL})]^{2+}$ (**1a**) is carried out, no intermediate species $[Cu_2(\text{H–XYL})(O_2)]^{2+}$ (**2a**) can be observed spectroscopically. We find that, in accord with the kinetics study (*vide supra*), the slowed rate of hydroxylation for electron-withdrawing R allows for bench-top monitoring (i.e., on a longer timescale) of $[Cu_2(\text{R–XYL})(O_2)]^{2+}$ production, further attesting to the kinetic stability of these dioxygen intermediates.

Thus, for the fluoro, cyano, and nitro complexes $[Cu_2(\text{R–XYL})]^{2+}$ (**1d–f**), R = F, CN, $NO_2$, strongly UV–visible absorbing complexes $[Cu_2(\text{R–XYL})(O_2)]^{2+}$ (**2d–f**) can be detected upon oxygenation of dicopper(I) precursors $[Cu_2(\text{R–XYL})]^{2+}$ (**1d–f**) at –80 °C in $CH_2Cl_2$. **1d–f** exhibit featureless spectra in the 315–900-nm region, but purple-brown dioxygen complexes **2d–f** all have a very intense band at ~360 nm, another strong absorption in the 430–440-nm range, plus a somewhat weaker band or shoulder at ~530 (Table 5). These spectra are very similar in pattern and intensity to that of $[Cu_2(\text{H–XYL})(O_2)]^{2+}$ (**2a**) (detected by low-temperature stopped-flow experiments),[5] suggesting that **2d–f** are also 1:1 $O_2$-adducts of these dinuclear complexes. In addition, these spectral features closely match those observed for $[Cu_2(Nn)(O_2)]^{2+}$, where Nn is a dinucleating ligand similar to XYL but having a variable methylene chain connecting the two PY2 tridentate chelators.[26]

The stability of $[Cu_2(\text{R–XYL})(O_2)]^{2+}$ (**2d–f**) is still somewhat limited, as indicated by the decrease in intensity of the absorptions with time (i.e., minutes to hours). Thus, the extinction coefficients given in Table 5 are approximate (±10–15%) and represent values determined for the maximum absorption observed, usually a few minutes after direct oxygenation (by bubbling) of precursors **1d–f**. The nitro complex $[Cu_2(NO_2\text{–XYL})(O_2)]^{2+}$ (**2f**), with the most electron-poor xylyl group, is the most stable of the three species, when handled in this manner. In fact, the reversible binding of $O_2$ and CO can be determined by the ability to remove $O_2$ from **2f** by application of a vacuum while quickly heating the $CH_2Cl_2$ solution, as has been carried out by other types of reversible dioxygen-carrying copper complexes.[1,2,26,35] While the behavior is not ideal, due to the instability of **2f** {which is either due to its thermal decomposition or follow-up hydroxylation giving $[Cu_2(NO_2\text{–XYL–O}^-)(OH)]^{2+}$ (**3f**)}, several oxygenation–deoxygenation cycles can be carried out and followed spectrophotometrically, as shown in Figure 4. "Carbonyl cycling" can also be effected,[18] where CO is used to displace $O_2$ from **2f**, giving $[Cu_2(NO_2\text{–XYL})(CO)_2]^{2+}$; carbon monoxide is removed from this by application of a vacuum at room temperature, producing $[Cu_2(NO_2\text{–XYL})]^{2+}$ (**1f**), and $[Cu_2(NO_2\text{–XYL})(O_2)]^{2+}$ (**2f**) is regenerated by oxygenation after chilling (–80 °C).

The more electron rich *tert*-butyl-substituted complex $[Cu_2(t\text{-Bu–XYL})]^{2+}$ (**1c**) reacts very rapidly with dioxygen, and at –80 °C, no strongly absorbing species $[Cu_2(t\text{-Bu–XYL})(O_2)]^{2+}$ (**2c**) can be observed in a bench-top spectroscopic experiment. We also confirmed that $[Cu_2(\text{MeO–XYL})]^{2+}$ (**1b**) does not react with $O_2$ at all at –80 °C, in spite of the fact that, at room temperature, oxygenation and facile hydroxylation occur to give the normal product $[Cu_2(\text{MeO–XYL–O}^-)(OH)]^{2+}$ (**3b**) (*vide supra*).

**Methoxo Analog $[Cu_2(\text{MeO–XYL})]^{2+}$ (1b): Variable-Temperature $^1$H NMR Studies of Complexes 1a–f.** As discussed, while the methoxo-substituted derivative $[Cu_2(\text{MeO–XYL})]^{2+}$ (**1b**) reacts with $O_2$ at room temperature to give the expected phenoxo- and hydroxo-bridged product $[Cu_2(\text{MeO–XYL–O}^-)(OH)]^{2+}$ (**3b**), there is no low-temperature oxygenation reaction, precluding a kinetic/thermodynamic analysis. The $^1$H NMR behavior with unusual negative CIS observations for **1b** (Table 1) points to this complex as having unique coordination characteristics, and this is substantiated by comparison of low-temperature $^1$H NMR spectra of the various dicopper(I) xylyl complexes **1a–f**.

---

(33) Zuberbühler, A. D.; Cruse, R. W.; Kaderli, S.; Meyer, C. J.; Karlin, K. D. *J. Am. Chem. Soc.* **1988**, *110*, 5020–5024.

(34) Karlin, K. D., and co-workers. Unpublished observations.

(35) Tyeklár, Z.; Jacobson, R. R.; Wei, N.; Murthy, N. N.; Zubieta, J.; Karlin, K. D. *J. Am. Chem. Soc.* **1993**, *115*, 2677–2689.

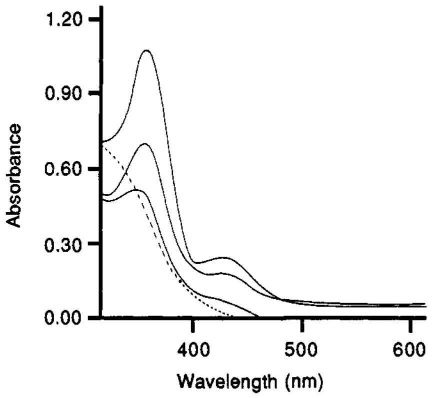

**Figure 4.** UV-visible spectra indicating the reversible nature of dioxygen binding to $[Cu_2(NO_2–XYL)]^{2+}$ (**1f**), via "vacuum-cycling" experiments. Bubbling $O_2$ through -80 °C solution of **1f** in $CH_2Cl_2$ (dotted line) produces $[Cu_2(NO_2–XYL)(O_2)]^{2+}$ (**2f**) (solid line, top). Application of a vacuum with brief heating removes the bound $O_2$, regenerating **1f** (not shown). Reoxygenation after cooling to -80 °C again gives **2f**, and this process can be repeated one more time, as shown. The loss in absorbance through each cycle is due to decomposition. See text for further explanation.

Figure 5 provides variable-temperature $^1H$ NMR spectra for $[Cu_2(MeO–XYL)]^{2+}$ (**1b**) and $[Cu_2(t\text{-Bu–XYL})]^{2+}$ (**1c**) in 20-deg intervals over the range -80 to -20 °C. The line width of the benzylic 1′-$CH_2$ resonance ($\delta \sim 3.7$ ppm; see Figure 1 for labeling scheme) for **1b** is observed to increase dramatically as one goes below -20 °C, and the peak essentially disappears into the baseline at ~ -40 °C. The next most affected resonances are the py-6″ protons (next to the pyridine N, $\delta \sim 8.5$ ppm). At -60 °C two new peaks in each of these regions appear, and these sharpen at still lower temperature, -80 °C. By contrast, the corresponding peaks for the *t*-Bu derivative **1c** are not broadened to any significant extent even down to -60 °C and show only a slight broadening at -80 °C (Figure 5). The latter similar behavior is also observed for the other 5-substituted complexes **1a,d–f** (not shown).[18]

Temperature-dependent NMR spectroscopic line broadening of the type seen for $[Cu_2(MeO–XYL)]^{2+}$ (**1b**) is most often thought to arise from two possible causes: (i) paramagnetic effects from impurities of Cu(II)[36] and (ii) exchange (dynamic) processes, which arise from either intramolecular motions and rearrangements or intermolecular exchanges, which may also broaden NMR signals if the exchange process occurs at a rate similar to the NMR time scale. Here, the consistency of the data and comparison of a series of related complexes indicate that dynamic processes are predominantly responsible for the observed line broadening, and paramagnetic effects can be ruled out.

A reasonable explanation of the data observed for the case of $[Cu_2(MeO–XYL)]^{2+}$ (**1b**) begins with the suggestion that at all temperatures there exists some interaction of the copper(I) ions with the methoxybenzene ring and that this accounts for the unusual CIS behavior; molecular models suggest that no interaction of copper ions with the atoms of the xylyl 5-substituents are possible. At room temperature and even down to -20 °C, the two Cu-chelate arms of the ligand are quickly changing position and thus chemically equivalent in solution (on the NMR time scale). Single resonances for the 1′-$CH_2$ ($\delta \sim 3.8$ ppm) and py-6″ $^1H$ NMR signals are observed, cf., Table S1 (supplementary material). Thus, the two protons on individual 1′-$CH_2$ methylene groups are chemically equivalent. The appearance of two widely separated 1′-$CH_2$ proton peaks ($\delta \sim 3.8$ and 4.5 ppm) upon lowering the temperature below -40 °C is interpreted to indicate that there is a freezing out or "locking" of the tricoordinate Cu-chelate arms, such that they are *not* free to rotate. The NMR data are consistent with the notion that this occurs in a symmetrical manner, since the methoxybenzene 4- and 6-protons do not split throughout the temperature range. Consistent with such symmetry, either both chelate arms (i.e., the Cu atoms) are on one side of the plane of the methoxybenzene moiety or they are on opposite sides. We favor the latter likelihood for the following reasons: (i) This situation corresponds more closely to the crystal structure of $[Cu_2(H–XYL)]^{2+}$ (**1a**)[6] as well as that of an analog in which all four pyridine donors contain a 6-methyl group;[17] in these, the two chelate arms are chemically equivalent and extended away from one another, on opposite sides of the xylyl spacer, such that the Cu···Cu distance is ~9 Å. (ii) This also would explain the lack of $O_2$-reactivity at low temperature, since the Cu(I) ions are not close enough to each other for the possibility of $O_2$-bridging between copper ions, this being necessary for formation of a $Cu_2O_2$ complex and subsequent reactivity.

In the "frozen" or locked low-temperature structure, the $\delta \sim 3.8$ and 4.5 ppm 1′-$CH_2$ signals represent pairs of hydrogen on different methylene groups, now in different chemical environments. Examinations of stick molecular models shows this very clearly. The freezing out makes the two pyridyl rings on a given chelate arm inequivalent, too, thus accounting for the clear splitting of the initially (i.e., at higher temperatures) equivalent py-6″ protons ($\delta \sim 8.45$ ppm, Table S1). As mentioned, these split into two sharp peaks at ~8.3 and 8.6 ppm (Figure 5). Other splittings are observed (Figure 5), but these are less easy to resolve or assign. In addition, a low-temperature $^{13}C$ NMR spectrum of $[Cu_2(MeO–XYL)]^{2+}$ (**1b**) exhibits more than the 13 $^{13}C$ resonances observed at room temperature (cf., Table S2);[34] these data were not further analyzed.

The unusual NMR behavior and concomitant lack of low-temperature $O_2$-reactivity only occurs for the methoxo analog $[Cu_2(MeO–XYL)]^{2+}$ (**1b**). As mentioned above, we suggest this may be due to an interaction of copper(I) ions in **1b** with the phenyl ring, which is electron rich because of the presence of the methoxy group. A "chelate effect" places the Cu(I) ions in **1b** in close proximity to the methoxybenzene ring, thus making a Cu(I)/$\pi$-phenyl interaction favorable. In addition, the Cu(I) ions are three-coordinate and thus "coordinatively" unsaturated.

Olefin coordination to copper(I) ion is quite common,[37–39] and one can cite a number of examples from the literature in which a benzene ring coordinates to copper(I) ions.[40–42]

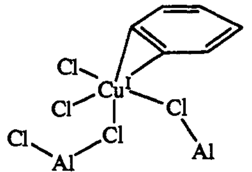

For example, in $C_6H_6CuAlCl_4$, the benzene ring forms a $\pi$-type bond with the copper through one carbon–carbon bond only and the plane of the benzene ring is above the copper atom.[40] Examination of stick molecular models suggests Cu(I) phenyl ring interactions are possible, for example, the Cu chelate off C1 (Figure 1) binding to the C2–C3 or to the C5–C6 arene bond, although binding to C3–C4 (or C4–C5) does not appear to be

---

(36) LaMar, G. N.; Horrocks, W. DeW., Jr.; Holm, R. H. *NMR of Paramagnetic Molecules*; Academic Press: New York, 1973.

(37) (a) Hathaway, B. J. In *Comprehensive Coordination Chemistry*; Wilkinson, G., Ed.; Pergamon Press: New York, 1987; Chapter 53, Vol. 5, pp 533–774. (b) Camus, A.; Marsich, N.; Nardin, G.; Randaccio, L. *Inorg. Chim. Acta* **1977**, *23*, 131–144.

(38) Thompson, J. S.; Whitney, J. F. *Inorg. Chem.* **1984**, *23*, 2813–2819.

(39) (a) Nelson, S. M.; Lavery, A.; Drew, M. G. B. *J. Chem. Soc., Dalton Trans.* **1986**, 911. (b) Sanyal, I.; Murthy, N. N.; Karlin, K. D. *Inorg. Chem.* **1993**, *32*, 5330–5337.

(40) Turner, R. W.; Amma, E. L. *J. Am. Chem. Soc.* **1963**, *85*, 4046.

(41) Pasquali, M.; Floriani, C.; Gaetani-Manfredotti, A. *Inorg. Chem.* **1980**, *19*, 1191.

(42) (a) Salomon, R. G.; Kochi, J. K. *J. Am. Chem. Soc.* **1973**, *95*, 1889–1897. (b) Dines, M. B.; Bird, P. H. *Chem. Commun.* **1973**, 12.

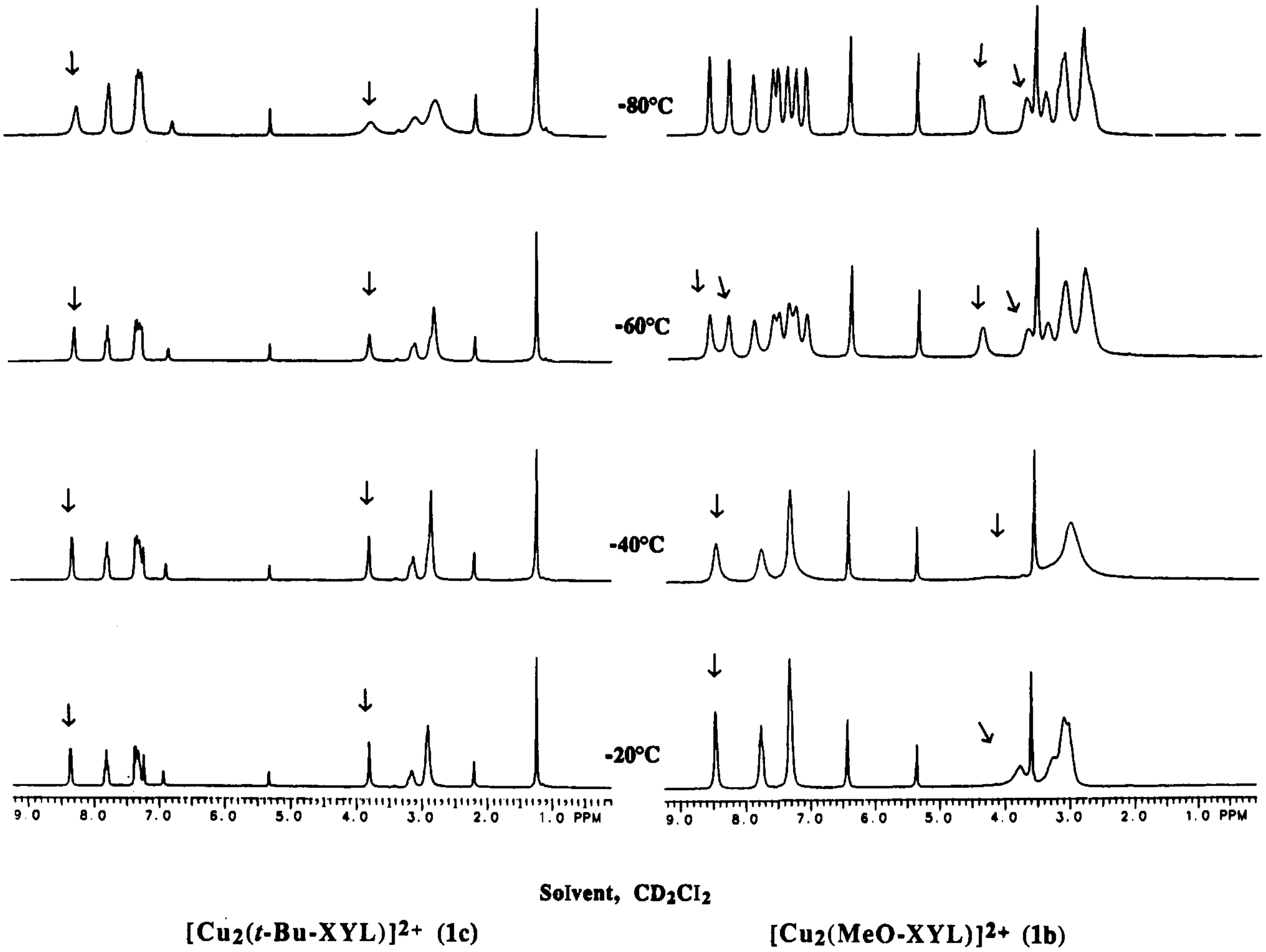

**Figure 5.** Variable-temperature $^1H$ NMR spectra for $[Cu_2(t\text{-Bu–XYL})]^{2+}$ (**1c**) and $[Cu_2(MeO\text{–XYL})]^{2+}$ (**1b**), demonstrating, in particular for **1b**, the freezing out of conformations of the chelating arms with decreasing temperature. The arrows indicate the peaks assigned to the 6″ pyridine protons (downfield) and the 1′ methylene protons (upfield).

precluded. An X-ray structure of $[\{Cu^I(CF_3SO_3^-)\}_2(\text{benzene})]$ shows that, in the polymeric structure observed, the arene is bound by two Cu(I) ions, one above and the other below.[42] An analogous π-interaction to the phenyl ring from both Cu(I) ions in $[Cu_2(MeO\text{–XYL})]^{2+}$ (**1b**) would appear to be consistent with the $^1H$ NMR spectra; the two pyridine rings of each arm would be chemically inequivalent, leading to the splitting of the 1′-$CH_2$ and py-6″ protons into groups of two, yet the 4,6 phenyl protons do not split or move much (Figure 5).

In conclusion, $[Cu_2(MeO\text{–XYL})]^{2+}$ (**1b**) possesses distinctive characteristics, observable by NMR spectroscopy. Interaction of three-coordinate Cu(I) with an electron-rich methoxybenzene would appear to explain most of the observed behavior, including the lack of reactivity with $O_2$ at low temperature. Specific confirmation of the detailed nature of the low-temperature interactions of solutions of **1b** could be subject for future consideration.

## Summary and Conclusions

Through detailed investigations involving the combination of synthesis, reactivity, spectroscopic probing, and low-temperature stopped-flow kinetic/thermodynamic inquiries, dioxygen reactions with dicopper(I) complexes $[Cu_2(R\text{–XYL})]^{2+}$ (**1**) have provided a wealth of new chemistry and information concerning fundamental aspects of interactions of $O_2$ with reduced copper(I), reversible binding, as well as C–H "activation", i.e., biomimetic hydroxylation mediated by copper–dioxygen chemistry. All of these aspects have been included in this report, which has emphasized systematic variation in the xylyl 5-substituent R, that para to the position being hydroxylated (Figure 1). In all cases, dioxygen reaction leads to hydroxylation of the xylyl group and formation of the phenoxo-bridged dicopper(II) complex $[Cu_2(R\text{–XYL–O}^-)(OH)]^{2+}$ (**3**); phenol O-atom incorporation from molecular oxygen has been proven.

Detailed kinetic/thermodynamic studies reinforce those concepts concerning $Cu(I)_n/O_2$ interactions that have only recently become apparent due to the considerable advances in the generation and characterization of discrete $Cu_2O_2$ complexes.[1-3,7-10] Dioxygen binding to Cu(I) is rapid and involves low activation enthalpies and large, negative activation entropies. Pseudo-reversible binding of $O_2$ to all dicopper(I) complexes $[Cu_2(R\text{–XYL})]^{2+}$ (**1**) is confirmed by the present kinetics investigation, and the driving force for the reaction is entirely given by enthalpy. As seen elsewhere[1,5,29] and here, the room temperature instability of $Cu_2O_2$ complexes is precluded by the highly unfavorable $\Delta S°_{\text{formation}}$, something that copper–proteins are able to overcome presumably by compensating for protein conformational changes.[29] Interestingly, the detailed pattern of kinetic and thermodynamic parameters observed would appear to suggest that the rather remote R-group influences $O_2$-binding and release, but this is seen as more likely to be due to the multistep nature of the processes involved. An important result coming from the present study is the dependence of $k_2$ upon R, i.e., how the rate of hydroxylation is influenced by the xylyl ring substituent in the intermediate $Cu_2O_2$ species $[Cu_2(R\text{–XYL})(O_2)]^{2+}$ (**2**). For example, the modest reduction of $k_2$ value at -90 °C for $[Cu_2(NO_2\text{–XYL})(O_2)]^{2+}$ (**2f**) [about 20× compared to that of **2a** (R = H)], in combination with changes in the other $k$ values (Table

3), allows for the direct low-temperature UV–visible observation of this particular $Cu_2O_2$ adduct, and even cycling between it and its deoxy form $[Cu_2(NO_2–XYL)]^{2+}$ (**1f**) is possible. While not overall a particularly strong substituent effect, electron-releasing substituents increase the rate of hydroxylation, providing corroborative evidence for the notion that the peroxo moiety in **2** is an electrophile.

The xylyl system described here serves as a functional mimic for copper hydroxylases, revealing both gross concepts as well as subtleties involved in reversible binding of dioxygen by a dicopper center where the two metal ions are not tightly linked and how such a center can activate $O_2$ for hydrocarbon oxidation under mild conditions, i.e., ≤1 atm external $O_2$-pressure and at room temperature or below. The extension of such notions to activation of dioxygen by other copper proteins which involve mono- or trinuclear copper centers[1–3,7–10,43,44] and well as the practical application to oxidative processes utilizing dioxygen are subjects for future consideration.

## Experimental Section

**Materials and Methods.** Reagents and solvents used were of commercially available reagent quality unless otherwise stated. Labeled dioxygen ($^{18}O_2$, 99%) was obtained from Icon Services, Inc. Dioxygen gas was dried initially by passing it through a short column of supported $P_4O_{10}$ (Aquasorb, Mallinkrodt) and was further dried by passing it through a copper coil tube immersed in a –80 °C cold trap. Methanol was distilled from $Mg(OMe)_2$, and anhydrous diethyl ether was obtained by passing it through a 50 cm long column of activated alumina or it was directly distilled from sodium/benzophenone under Ar. Dichloromethane was stirred with concentrated sulfuric acid for several days. After being washed with water, $Na_2CO_3$ (saturated) solution, and then water again, it was dried over anhydrous $MgSO_4$ for several days. Finally, it was refluxed and distilled from $CaH_2$ in the absence of light.

Preparations and handling of air-sensitive materials were carried out under an argon atmosphere using standard Schlenk techniques. Deoxygenation of solvents and solutions was effected by either repeated vacuum/purge cycles using argon or by bubbling (20 min) of Ar directly through the solutions. Solid samples were stored and transferred, and samples for IR and NMR spectra were prepared in a Vacuum/Atmospheres drybox filled with argon. Elemental analyses were performed by Desert Analytics, Tuscon, AZ.

Infrared spectra were recorded as Nujol mulls either on a Perkin-Elmer 710B or Perkin-Elmer 283 instrument. $^1H$ NMR spectra were measured in $CD_3NO_2$, $CD_3CN$, $CD_2Cl_2$, or $CDCl_3$ on either a Varian EM360 (60 MHz) or a Varian XL-300 (300 MHz) NMR spectrometer. $^{13}C$ NMR spectra were recorded in $CD_3NO_2$, $CD_2Cl_2$, or $CDCl_3$ on a Varian XL-300 (300 MHz) NMR spectrometer with broad-band proton decoupling. All the spectra were recorded in 5 mm o.d. NMR sample tubes (Norell). Chemical shifts are reported as $\delta$ values downfield from an internal standard of $Me_4Si$. Electrical conductivity measurements were carried out in DMF using a Barnstead Sybron Corporation Model PM-70CB conductivity bridge, using a Yellow Springs Instrument Co. Inc. 3403 cell. The cell constant, *k*, was determined using a standard aqueous KCl solution. Room-temperature magnetic moments were determined using a Johnson Matthey magnetic susceptibility balance, calibrated using $Hg[Co(SCN)_4]$. Electronic absorption spectra at room temperature were recorded on a Shimadzu UV-160 spectrometer in acetonitrile. As previously described,[45a] low-temperature electronic spectroscopic studies were carried out in dichloromethane on a Perkin-Elmer Lambda Array 3840 spectrophotometer driven by an IBM PC. Field desorption mass spectra were obtained at the General Electric Company, Schenectady, NY.

**Synthesis of Ligands. A. MeO–XYL.** 5-MeO–*m*-xylene (15.72 g, 0.12 mol) was brominated by refluxing with NBS (50 g, 0.28 mol) in 300 mL of $CCl_4$ for 5 h in the presence of trace amounts of benzoyl peroxide. In addition a 150-W bulb was used as a source of UV light. After cooling and filtering, the solvent was removed to give a crude oil. Recrystallization from 100 mL of $CCl_4$ and 200 mL of hexane while standing at 0 °C for 2 days resulted in the isolation of 5-MeO-1,3-bis(bromomethyl)benzene (7.0 g, 20%) as an off-white crystalline material. $^1H$ NMR ($CDCl_3$; $\delta$): 3.9 (s, 3 H, O-Me), 4.8 (s, 4 H, $CH_2$), 6.8–7.1 (3 H, aromatic).

This product (3.6 g, 12.2 mmol) was added to a solution of PY2[45] (6.4 g, 28 mmol) and triethylamine (4 g, 39 mmol) in 150 mL of ethyl acetate solution. This reaction mixture was stirred at room temperature for 4 days, whereupon the mixture was filtered and the solvent was removed to give a crude oil. This oil was chromatographed on $Al_2O_3$ with 100% ethyl acetate ($R_f$ = 0.40) to give 2 g (28%) of pure product, MeO–XYL.

**B. *t*-Bu–XYL.** Bromination of the compound 5-*t*-Bu–*m*-xylene (10 g, 0.06 mol) was carried out by refluxing in $CCl_4$ (75 mL) for 3 h with NBS (21.97 g, 0.12 mol) in the presence of a trace of benzoyl peroxide. After 3 h, the mixture was cooled and filtered and the solvent was removed *in vacuo* to give a crude oil. Recrystallization while standing at 0 °C for 3 days from $CCl_4$ (50 mL) and hexane (150 mL) resulted in the isolation of 1,3-bis(bromomethyl)-5-*tert*-butylbenzene as a crystalline solid (6.14 g, 31%). $^1H$ NMR ($CDCl_3$; $\delta$): 1.3 (s, 9 H), 4.35 (s, 4 H), 7.25 (m, 3 H).

This compound (1.41 g, 4.4 mmol) was added to a solution of PY2 (2.0 g, 8.8 mmol) and $Et_3N$ (1.42 g, 14.1 mmol) in 80 mL of ethyl acetate solution. The mixture was allowed to stir at room temperature for 5 days, whereupon the solution was filtered and removal of the solvent from the filtrate gave a crude oil (3.16 g). This oil was chromatographed on alumina with 100% ethyl acetate ($R_f$ = 0.29), and a total of 1.45 g of pure product, *t*-Bu–XYL, was recovered (54%). MS (*m/z*): 613 (M + $H^+$), (*t*-Bu–XYL).

**C. F–XYL.** A 500-mL conical flask was charged with 40 mL of concentrated HCl and 40 mL of distilled water, the reaction mixture was cooled to 0 °C, and 3,5-dimethylaniline (20 g, 0.165 mol) was added with stirring into this ice-cooled mixture. Thick, solid precipitates of hydrochloride salt were formed which were dissolved by adding 25 mL of an aqueous solution of $NaNO_2$ (12 g, 0.17 mol) with stirring, while maintaining the temperature at 0–5 °C. Meanwhile 50 mL of a water solution of $NaBF_4$ (25.3 g, 0.23 mol) was cooled in ice and added to the above solution with stirring. The thick slurry was filtered with a Buchner funnel using Whatman filter paper. The precipitates were washed with 15 mL of ice water, 10 mL of methanol, and then 20 mL of ether. The solid was dried at room temperature and heated gently in a 250-mL round-bottomed flask inside an efficient hood. At the end, the flask was heated strongly and the residue was vacuum-distilled (~115 °C) to give 8.5 g (41%) of pure 5-fluoro-*m*-xylene. $^1H$ NMR ($CDCl_3$; $\delta$): 1.8 (s, 6 H), 5.9 (s, 1 H), 6.1 (s, 2 H). MS (*m/z*): 124.

Bromination of above compound (6 g, 0.05 mol) was carried out by refluxing in $CCl_4$ (200 mL) for 24 h with NBS (17.8 g, 0.1 mol) in the presence of a trace of benzoyl peroxide. In addition a 150-W light bulb was also applied for 10 h. The mixture was cooled and filtered, and the solvent was removed *in vacuo* to give a crude oil. Recrystallization while standing at 0 °C for 2 days from $CCl_4$ (40 mL) and hexane (60 mL) resulted in the isolation of 1,3-bis(bromomethyl)-5-fluorobenzene (4 g, 30%) as a crystalline solid. $^1H$ NMR ($CDCl_3$; $\delta$): 4.25 (s, 4 H, $CH_2Br$), 5.8–7.0 (m, 3 H).

This bis-bromo product (3.67 g, 13.34 mmol) was mixed with a solution of PY2 (7 g, 30 mmol) and $Et_3N$ (4 g, 40 mmol) in 100 mL of ethyl acetate. The mixture was stirred at room temperature for 5 days and filtered, and the filtrate was concentrated to give a crude oil. This oil was chromatographed on $Al_2O_3$ using ethyl acetate ($R_f$ ~ 0.43) to give pure product, F–XYL (5.1 g, 66%). $^{19}F$ NMR ($CD_3NO_2$; $\delta$, $CFCl_3$): –114.8. MS (*m/z*): 574 (M + $H^+$).

**D. CN–XYL.** KCN (25 g, 0.39 mol) was mixed with $Cu^ICN$ (18 g, 0.2 mol) in 100 mL of distilled water in a 1000-mL round-bottomed flask and gently heated to 40–50 °C with stirring. A 500-mL conical flask was charged with 40 mL of concentrated HCl and 40 mL of distilled water, the reaction mixture was cooled to 0 °C, and 3,5-dimethylaniline (20 g, 0.165 mol) was added with stirring into this ice-cooled mixture. The thick precipitates formed were dissolved by slowly adding 25 mL of an aqueous solution of $NaNO_2$ (12 g, 0.17 mol) and neutralized by adding 15 g of anhydrous $Na_2CO_3$ very slowly. The temperature was maintained at ~0 °C duirng all these steps. This solution was added slowly to the above $Cu^ICN$ solution, while the temperature was maintained between 60 and 70 °C. The solution was refluxed for 0.5 h to complete the reaction

---

(43) Ascorbate oxidase and laccase are multicopper oxidases, reducing $O_2$ to $H_2O$ at a trinuclear copper-containing active site. See refs 7–9 and: Messerschmidt, A.; Ladenstein, R.; Huber, R.; Bolognesi, M.; Avigliano, L.; Petruzzelli, R.; Rossi, A.; Finazzi-Agrò, A. *J. Mol. Biol.* **1992**, *224*, 179–205.

(44) A recent report suggests that the membrane-bound fraction of the methanotrophic enzyme methane monooxygenase is a copper enzyme, with a trinuclear active-site core: Chan, S. I.; Nguyen, H.-H. T.; Shiemke, A. K.; Lidstrom, M. E. In ref 7, pp 184–195.

(45) (a) Nelson, S. M.; Rodgers, J. *Inorg. Chem.* **1967**, *6*, 1390–1395. (b) Romary, J. K.; Zachariasen, R. D.; Garger, J. D.; Schiesser, H. *J. Chem. Soc. C* **1968**, 2884–2887.

and steam distilled. The receiving flask was cooled to ~10 °C, and the solution was filtered to get a yellowish brown solid. Recrystallization from a saturated solution in ethyl alcohol while keeping at 0 °C for 12 h gave 6 g (28%) of pure compound. $^1$H NMR ($CDCl_3$; δ): 2.4 (s, 6 H), 7.1 (s, 3 H). IR (Nujol; cm$^{-1}$): 2240 (s, CN), 1600 (C=C, aromatic).

Bromination of the above compound (4 g, 0.03 mol) was carried out by refluxing in $CCl_4$ (250 mL) for 24 h with NBS (10.89 g, 0.06 mol) in the presence of trace amounts of benzoyl peroxide. In addition a 150-W light bulb was also used. The mixture was cooled and filtered, and the filtrate was concentrated to give a thick oily material. Recrystallization from $CCl_4$ (30 mL) and hexane (50 mL), while keeping at 0 °C for 2 days, gave 1,3-bis(bromomethyl)-5-cyanobenzene (3.4 g, 37%). $^1$H NMR ($CDCl_3$; δ): 4.3 (s, 4 H), 7.4 (s, 3 H).

This product (3.4 g, 0.012 mol) was reacted with a solution of PY2 (5.87 g, 0.025 mol) and $Et_3N$ (3.73 g, 0.037 mol) in 150 mL of ethyl acetate. The mixture was allowed to stir at room temperature for 4 days, whereupon the mixture was filtered and the solvent was removed to give a crude oil. Chromatography on $Al_2O_3$ using ethyl acetate ($R_f$ = 0.4) gave pure product, CN–XYL (2.15 g, 45%). MS (*m/z*): 582 (M + H$^+$).

E. **$NO_2$–XYL.** Bromination of the compound, 5-nitro-*m*-xylene (10 g, 0.07 mol) was carried out by refluxing in $CCl_4$ (60 mL) for 24 h with NBS (23.6 g, 0.13 mol) in the presence of a trace of dibenzoyl peroxide. In addition, a 150-W light bulb was used. After 24 h the mixture was cooled and filtered and the solvent was removed *in vacuo* to give an oily residue. Recrystallization while standing at 0 °C for 3 days from $CCl_4$ (20 mL) and hexane (100 mL) resulted in the isolation of off-white crystalline 1,3-bis(bromomethyl)-5-nitrobenzene (5.74 g, 28%). $^1$H NMR ($CDCl_3$; δ): 8.14 (s, 2 H), 7.71 (s, 1 H), 4.5 (s, 4 H). Mp: 102–104 °C.

The above compound (0.34 g, 1.1 mmol) was added to a solution of PY2 (0.50 g, 2.2 mmol) and $Et_3N$ (0.36 g, 2.5 mmol) in 75 mL of ethyl acetate solution. The mixture was allowed to stir at room temperature for 5 days, whereupon the solution was filtered and removal of the solvent gave a crude oil. This oil was chromatographed on $Al_2O_3$ with ethyl acetate ($R_f$ = 0.54), and a total of 0.36 g (54%) of pure product, $NO_2$–XYL, was recovered. IR (neat film; cm$^{-1}$): ca. 3400 (br, s, $H_2O$), ca. 2900 (s, C—H), 2200 (m), 1615 (s, C=C), 1565 (s, $NO_2$ asymmetric), 1530 (s, $NO_2$ asymmetric), 1350 (s, br, $NO_2$ symmetric). MS (*m/z*): 602 (M + H$^+$).

F. **5-Ethyl-2-vinylpyridine.** This compound was prepared by a modification of the procedure described in the literature.[46] In a 1-L one-neck round-bottomed flask, 500 g (4.126 mol) of 5-ethyl-2-methylpyridine, 185.7 g (6.2 mol) of paraformaldehyde, and 150 mL of ethyl alcohol were placed along with 10 mL of formic acid and 0.2 g of *tert*-butylcatechol (as stabilizer). The mixture was refluxed with stirring for 5 days and steam distilled to remove the solvent and excess starting material. The residue was extracted with two (200-mL) portions of chloroform, and the solvent was removed by rotary evaporation to give 250 mL of thick liquid 5-ethyl-2-(2-hydroxyethyl)pyridine. $^1$H NMR (60 MHz) using $CDCl_3$ as solvent δ: 1.2 (t, 3 H), 2.5 (q, t, 6 H), 6.8–7.4 (m, 2 H), 8.2 (d, br, 1 H(py-6)). This was placed in a 500-mL two-neck round-bottomed flask, and 150 g of KOH was added. To one neck was attached a distillation apparatus, and to the other neck, an air-tight dropping funnel containing 5-ethyl-2-(2-hydroxyethyl)pyridine. This was added dropwise while heating the flask, and a total of 140 g (1.05 mol) of 5-ethyl-2-vinylpyridine was collected (25%) at 110–120 °C under 0.2 mmHg pressure. $^1$H NMR (60 MHz) ($CDCl_3$; δ): 1.3 (t, 3 H), 2.5 (q, 2 H), 5.1–5.3 (d of d, 1 H), 5.7–6.2 (d of d, 1 H), 6.3–6.7 (t, 1 H), 6.8–7.2 (m, 2 H, py), 8.1 (s, b, 1 H, py).

G. **H–XYL–(5-Et–PY)$_2$.** In a 500-mL round-bottomed flask, a mixture of 17 g (0.125 mol) of *m*-xylenediamine and 100 g (0.752 mol) of 5-ethyl-2-vinylpyridine was added by dissolving in 30 mL of methanol. The resultant solution was refluxed for 7 days with stirring in the presence of 37.5 g (0.625 mol) of acetic acid as a catalyst. The solution was cooled to room temperature, and solvent was removed by rotary evaporation. The resulting oil was dissolved in 300 mL of $CH_2Cl_2$ and washed once with 200 mL of 15% NaOH(aq) and two times with distilled water, before it was dried using $MgSO_4$. The solution was filtered, and solvent was removed by rotary evaporation to give a crude oil (80 g). Fifteen grams of this oil was chromatographed on a 45 × 5 cm$^2$ glass column packed with $Al_2O_3$ up to a 20-cm height. In the beginning pure diethyl ether was used as the eluant to remove all the excess 5-ethyl-2-vinylpyridine. Then, ethyl acetate was used, and fractions of pure product were collected ($R_f$ = 0.45), combined, and concentrated by removing the solvent by rotary evaporation. The light green-yellow oil obtained was dissolved in 200 mL of $CH_2Cl_2$, the resulting solution was dried with $MgSO_4$ and filtered on a fast-speed filter paper, and the solvent was removed by rotary evaporation to give 3 g of pure product. In this way all the crude oil was chromatographed to give a total of 15 g (0.022 mol, 18%) of product. IR (neat film; cm$^{-1}$) ca 3400 (br, s, $H_2O$), ca. 2900 (s, C—H), 1680 (m, $H_2O$), 1600 (s, C=C), 1560 (s).

H. **Bis(2-(2-(5-Et-pyridyl))ethyl)amine.** In a 500-mL round-bottomed flask, 57 g (0.428 mol) of 5-ethyl-2-vinylpyridine and 45.8 g (0.857 mol) of $NH_4Cl$ were mixed along with 50 mL each of methanol and water. The mixture was refluxed with stirring for 2 days and concentrated on a rotary evaporator to remove methanol. The solid slurry was dissolved in 200 mL of dichloromethane and washed once with 10% (6 g) NaOH solution and twice with distilled water. The $CH_2Cl_2$ layer was dried with $MgSO_4$, filtered, and concentrated by rotary evaporation. The thick oil obtained was chromatographed on a 5 × 40 cm$^2$ column packed with $Al_2O_3$. First, the column was eluted with diethyl ether to remove excess 5-ethyl-2-vinylpyridine, after which it was eluted with 100% ethyl acetate to remove any tertiary amine. The fractions of pure product were chromatographed (EtOAc/MeOH, 9:1) ($R_f$ = 0.4, $Al_2O_3$ plates, solvent ethyl acetate/methanol = 9/1), collected, and combined, whereupon the solvent was removed by rotary evaporation. The concentrate was dissolved in 150 mL of $CH_2Cl_2$, and the resulting solution was dried over $MgSO_4$, filtered through a Whatman filter paper, and rotary evaporated to give 10 g (0.35 mol) of product (16.5%). $^1$H NMR (60 MHz) ($CDCl_3$, δ) 1.0–1.3 (t, 6 H, 5″(b)), 2.3–2.7 (q, 4 H, 5″(a)), 2.75–3.0 (s, b, 8 H, 1′ + 2′), 6.75–7.3 (m, 4 H, py-3″ + 4″), 8.1 (2 H, py-6″).

I. **$NO_2$–XYL–(5-Et–PY).** The compounds 1,3-bis(bromomethyl)-5-nitrobenzene[47] (1 g, 3.23 mmol) and bis(2-(2-(5-Et–pyridyl))ethyl)amine (1.86 g, 6.6 mmol) were mixed in 100 mL of ethyl acetate and stirred for 0.5 h at 0 °C in an ice bath. After that triethylamine (1 g, 9.9 mmol) was added slowly and the solution was brought to room temperature. The mixture was stirred at room temperature for 5 days, after which the resultant mixture was filtered and concentrated by rotary evaporation to give 2.8 g of crude oil. This oil was chromatographed on a 20 × 3.8 cm$^2$ wide glass column packed with $Al_2O_3$. The compound was eluted with 100% ethyl acetate, and pure fractions with $R_f$ = 0.65 were collected, combined, and concentrated by rotary evaporation. The residue was dissolved in $CH_2Cl_2$ (150 mL) and dried with $MgSO_4$, and 0.8 g (1.12 mmol, 34%) of pure compound was obtained after removing the solvent.

**Synthesis of Cu(I) and Cu(II) Complexes.** The number of fraction of solvate molecules given for copper complex formulations is based on (i) $^1$H NMR integration and (ii) fitting to C, H, and N combustion analyses, and it is therefore approximate.

A. **$[Cu^I_2(MeO–XYL)](PF_6)_2 \cdot 0.75CH_2Cl_2$ (1b-$(PF_6)_2$).** A 25-mL $CH_2Cl_2$ solution of the ligand, MeO–XYL (0.4 g, 0.68 mmol) was stirred with $[Cu^I(CH_3CN)_4]PF_6$ (0.51 g, 1.36 mmol) for 0.5 h under argon. The resultant solution was filtered through a medium-porosity frit and precipitated with 50 mL of ether. Liquid was decanted, and solid was vacuum-dried to give 0.48 g (66%) of an off-white powder. Anal. Calcd for $C_{37.75}H_{43.5}N_6Cu_2Cl_{1.5}F_{12}OP_2$: C, 42.46; H, 4.07; N, 7.87. Found: C, 42.36; H, 4.00; N, 8.13. IR (Nujol; cm$^{-1}$) 1600 (C=C, aromatic), 840 ($PF_6$).

B. **$[Cu^I_2(t\text{-}Bu–XYL)](PF_6)_2 \cdot 1.5CH_2Cl_2$ (1c-$(PF_6)_2$).** A 30-mL $CH_2Cl_2$ solution of compound *t*-Bu–XYL (0.3 g, 0.49 mmol) was stirred with $[Cu^I(CH_3CN)_4]PF_6$ (0.37 g, 0.98 mmol) under Ar. After 0.5 h, the product was precipitated with 100 mL of ether. The liquid was decanted, and the solid was again dissolved in 40 mL of $CH_2Cl_2$, filtered through a medium-porosity frit, and precipitated with 150 mL of ether. The liquid was decanted, and solid was dried under vacuum overnight to give 0.42 g (74%) of a yellowish brown solid. Anal. Calcd for $C_{41.5}H_{51}N_6Cu_2Cl_3F_{12}P_2$: C, 43.69; H, 4.46; N, 7.28. Found: C, 42.72; H, 4.55; N, 7.77. IR (Nujol; cm$^{-1}$) of 2900 (C—H), 1600 (C=C), 840 (s, br, $PF_6$).

C. **$[Cu^I_2(F–XYL)](PF_6)_2 \cdot 1CH_3CN$ (1d-$(PF_6)_2$).** To a 20-mL acetonitrile solution of $[Cu^I(CH_3CN)_4]PF_6$ (3 g, 8 mmol) was added dropwise F–XYL (2.60 g, 4.5 mmol) dissolved in 35 mL of acetonitrile. After 30 min of stirring, the solution was filtered and precipitated with 150 mL of ether. The liquid was decanted, and the solid was vacuum-dried overnight to give 2.8 g (68%) of pure material. Anal. Calcd for $C_{38}H_{42}N_7Cu_2F_{13}P_2$: C, 44.20; H, 4.06; N, 9.49. Found: C, 44.70; H, 4.20; N, 9.49. IR (Nujol; cm$^{-1}$): 1600 (C=C, aromatic), 840 ($PF_6$).

---

(46) Kauffman, H. F. Ir. U.S. Patent 2556845, June 12, 1951.

(47) (a) Kazuhiko, S.; Lin, R. J.; Masataka, K.; Masaki, H. *J. Am. Chem. Soc.* **1986**, *108*, 1916. (b) Sherrod, S. A.; de Costa, R. L.; Barnes, R. A.; Boekelheide, V. *J. Am. Chem. Soc.* **1974**, *96*, 1565.

**D. $[Cu^I_2(CN–XYL)](PF_6)_2·0.2CH_3CN$ (1e-$(PF_6)_2$).** To a 15-mL acetonitrile solution of $[Cu^I(CH_3CN)_4]PF_6$ (0.63 g, 1.7 mmol) was added dropwise CN–XYL (0.5 g, 0.86 mmol) dissolved in 15 mL of acetonitrile. After 30 min of stirring, the solution was filtered and precipitated with 60 mL of ether. The liquid was decanted, and the solid was vacuum-dried overnight to give 0.68 g (79%) of a light-yellow powder. Anal. Calcd for $C_{37.4}H_{39.6}N_{7.2}Cu_2F_{12}P_2$: C, 44.60; H, 3.93; N, 10.01. Found: C, 43.99; H, 4.00; N, 10.21. IR (Nujol; cm$^{-1}$): 2260 (CN), 1600 (C=C, aromatic), 840 ($PF_6$).

**E. $[Cu^I_2(NO_2–XYL)](PF_6)_2·2CH_2Cl_2$ (1f-$(PF_6)_2$).** A 40-mL $CH_2Cl_2$ solution of compound $NO_2$–XYL (0.3 g, 0.54 mmol) was stirred with $[Cu^I(CH_3CN)_4]PF_6$ (0.37 g, 1.0 mmol) under Ar for 0.5 h. The resultant solution was precipitated with 100 mL of ether. The liquid was decanted, and the solid was again dissolved in 35 mL of $CH_2Cl_2$, filtered through a medium-porosity frit, and precipitated with 150 mL of ether. The liquid was decanted, and the solid obtained was vacuum-dried to give 0.38 g (64%) of pure yellow compound. Anal. Calcd for $C_{38}H_{43}N_7Cu_2Cl_4F_{12}O_2P_2$: C, 38.38; H, 3.66; N, 8.25. Found: C, 38.09; H, 4.12; N, 8.18. IR (Nujol; cm$^{-1}$): 1610 (C=C, aromatic), 1580 (w, $NO_2$ asymmetric), 1520 ($NO_2$ asymmetric), 1380 (s, $NO_2$ symmetric), 840 ($PF_6$).

**F. $[Cu^I_2(H–XYL–(5\text{-}Et–PY))](PF_6)_2·0.5CH_2Cl_2$ (1g-$(PF_6)_2$).** To a 250-mL Schlenk flask was added $[Cu(CH_3CN)_4]PF_6$ (1.04 g, 2.8 mmol), and a 250-mL addition funnel was attached via a 24/40 joint. The whole system was evacuated and purged with Ar four times, and a 40-mL $CH_2Cl_2$ solution of compound (1 g, 1.4 mmol) was bubbled with Ar for 20 min inside the addition funnel. This was added to the solid Cu(I) salt with stirring, after which a yellow solution was formed. After the addition of 40 mL of ether with stirring, the solution was filtered through a medium-porosity frit into another 200-mL Schlenk flask under Ar. Again a 250-mL addition funnel was attached to the flask, and 150 mL of ether was added to this clear, yellow solution. A yellow precipitate formed, which was washed with 100 mL of deaerated ether and vacuum-dried overnight to give 1.2 g (78%) of yellow powder. Anal. Calcd for $Cu_2C_{44.5}H_{57}ClN_6P_2F_{12}$: C, 47.40; H, 5.05; N, 7.45. Found: C, 47.73; H, 5.16; N, 7.37. IR (Nujol; cm$^{-1}$): 1600 (C=C, aromatic), 840 (br, $PF_6$).

**G. $[Cu^I_2(NO_2–XYL–(5Et\text{-}PY))](PF_6)_2·0.5CH_2Cl_2$ (1h-$(PF_6)_2$).** In a 100-mL Schlenk flask was added 0.417 g (1.12 mmol) $[Cu(CH_3CN)_4]PF_6$ and a magnetic stir bar. A 100-mL addition funnel (Kontes K-215200) was attached to a flask via a standard 19/22 joint. The whole system was evacuated and purged with Ar three times, and a 20-mL $CH_2Cl_2$ solution of $NO_2$-XYL-(5Et-PY) (0.4 g, 0.56 mmol) was added into the addition funnel under Ar. This solution was bubbled with Ar for 15 minutes and added to the solid $[Cu(CH_3CN)_4]PF_6$. Meanwhile 20 mL of ether was also bubbled with Ar in the addition funnel, and after this was added to the above yellow solution, the mixture was filtered under Ar through a medium-porosity frit into another 200-mL Schlenk flask which was first evacuated and purged with Ar. Ether (100 mL) was slowly added while the temperature was lowered to ~ −60 °C. A yellow precipitate settled out, the clear liquid was decanted under Ar, and the solid was washed with 50 mL of ether and vacuum-dried to give 0.5 g (80%) of yellow powder. Anal. Calcd for $Cu_2C_{44.5}H_{56}ClP_2F_{12}N_7O_2$: C, 45.54; H, 4.77; N, 8.35. Found: C, 45.82; H, 4.95; N, 8.11. IR (Nujol; cm$^{-1}$): 1540 (s, $NO_2$), 1370 (s, $NO_2$, symmetric), 840 (s, br, $PF_6$).

**H. $[Cu^{II}_2(MeO–XYL–O^-)(OH)](PF_6)_2$ (3b-$(PF_6)_2$).** Complex **1b** (0.51 g, 0.48 mmol) was stirred for 0.5 in 75 mL of Ar-saturated DMF. The temperature was lowered to 0 °C in ice, and the solution was exposed to dry oxygen for 24 h. The solvent was removed by high-vacuum rotary evaporation, and the brown residue was dissolved in 40 mL of $CH_2Cl_2$, filtered, and precipiated with 150 mL of ether. Liquid was decanted and solid dried to give 0.38 g (76%) of purple compound. Anal. Calcd for $C_{37}H_{42}N_6Cu_2F_{12}O_3P_2$: C, 42.89; H, 4.05; N, 8.11. Found: C, 42.72; H, 3.93; N, 7.77. Ligand analysis after extraction from the complex, TLC in 100% ethyl acetate/$Al_2O_3$: $R_f$ = 0.15; original ligand $R_f$ = 0.40. $^1H$ NMR ($CDCl_3$, $\delta$) of extracted ligand: 2.90 (s, 16 H), 3.5 (s, 3 H), 3.6 (s, 4 H), 286 (sh, 4940), 377 (2200), 638 (110).

**I. $[Cu^{II}_2(t\text{-}Bu–XYL–O^-)(OH)](PF_6)_2$ (3c-$(PF_6)_2$).** Complex **1c** (0.47 g, 0.4 mmol) was dissolved in 80 mL of DMF under Ar. The solution was stirred for 0.5 h at 0 °C and then exposed to an atmosphere of dry oxygen overnight. The solvent was removed by high-vacuum rotary evaporation, and the green residue was dissolved in 40 mL of $CH_2Cl_2$. After precipitation with 150 mL of ether, the solid was recrystallized from $CH_2Cl_2$/ether (30/70) to give 0.35 g (81%) of air-dried pure compound. Anal. Calcd for $C_{40}H_{48}N_6Cu_2F_{12}O_2P_2$: C, 45.22; H, 4.57; N, 7.91. Found: C, 45.21; H, 4.46; N, 7.72. Molar conductivity: 134.0 $\Omega^{-1}$ cm$^2$ mol$^{-1}$. EPR ($CHCl_3$/DMF (1:1), 77 K): "silent".

**J. Oxygenation of 1c-$(PF_6)_2$ using $^{18}O_2$.** Complex **1c-$(PF_6)_2$** (0.22 g, 0.19 mmol) was dissolved in DMF (40 mL) under argon. The solution was then exposed to $^{18}O_2$ for 18 h, while stirring at 0 °C. DMF was evaporated under reduced pressure, and the green residue was dissolved in 50 mL of $CH_2Cl_2$. The solution was extracted by stirring with 50 mL of $NH_4OH$. The extracted $CH_2Cl_2$ solution was concentrated, and the crude oil was chromatographed on silica using methanol ($R_f$ = 0.33) to give 0.09 g (74%) of pure product (*t*-Bu–XYL–OH (with $^{18}O_2$)). MS (*m*/*z*): 630 ($MH^+$), indicates ~94% incorporation of one $^{18}O$ atom into this phenol.

**K. $[Cu^{II}_2(F–XYL–O^-)(OH)](PF_6)_2·0.5CH_3CN$ (3d-$(PF_6)_2$).** Complex **1d-$(PF_6)_2$** (0.5 g, 0.48 mmol) was dissolved in 50 mL of DMF under Ar. The yellow solution was cooled to 0 °C and exposed to an atmosphere of dry oxygen overnight. Solvent was evaporated under reduced pressure, and the green residue was recrystallized from $CH_3CN$ (25 mL) and ether (100 mL) while keeping at 0 °C for 4 days, giving 0.43 g (85%) of dark-green air-dried crystals. Anal. Calcd for $C_{37}H_{40.5}N_{6.5}Cu_2F_{13}O_2P_2$: C, 42.54; H, 3.88; N, 8.72. Found: C, 42.50; H, 3.94; N, 9.17. TLC of extracted ligand ($Al_2O_3$/ethyl acetate): $R_f$ = 0.2; original ligand, i.e., F–XYL, $R_f$ = 0.45.

$^1H$ NMR spectroscopy was used to see the presence of $CH_3CN$ in this complex. The complex **3d-$(PF_6)_2$** (0.12 g, 0.11 mmol) was stirred in 2 mL of $CD_3NO_2$ for 4 h in a small test tube along with KCN (0.07 g, 1.1 mmol) as a reductant. A yellowish brown solution was formed, which was taken for NMR analysis. $^1H$ NMR (60 MHz) ($CD_3NO_2$; $\delta$): 1.98 (s, $CH_3CN$), 2.8 (s, br, 16 H), 3.4 (s, br, 4 H), 6.4–7.4 (m, 15 H), 8.1–8.3 (4 H, 6″).

**L. $[Cu^{II}_2(CN–XYL–O^-)(OH)](PF_6)_2$ (3e-$(PF_6)_2$).** Complex **1e-$(PF_6)_2$** (0.42 g, 0.41 mmol) was dissolved in 60 mL of DMF under Ar. The solution was stirred for 0.5 h at 0 °C and then exposed to an atmosphere of dry oxygen overnight. The solvent was removed by high-vacuum rotary evaporation, and the green residue was dissolved in 20 mL of $CH_3CN$, filtered, and layered with 60 mL of diethyl ether. Dark-green crystals were obtained upon standing at 0 °C for 1 week. The crystals were washed with 50 mL of ether and air-dried to give 0.28 g (65%) of pure compound. Anal. Calcd for $C_{37}H_{39}N_7Cu_2F_{12}O_2P_2$: C, 43.10; H, 3.78; N, 9.51. Found: C, 43.42; H, 3.77; N, 9.95. Analysis of extracted ligand, TLC ($Al_2O_3$/ethyl acetate): $R_f$ = 0.20; original ligand, i.e., CN–XYL $R_f$ = 0.4. MS (*m*/*z*): 598 ($MH^+$).

**M. $[Cu^{II}_2(NO_2–XYL–O^-)(OH)](PF_6)_2$ (3f-$(PF_6)_2$).** Complex **1f-$(PF_6)_2$** (0.46 g, 0.39 mmol) was dissolved in 80 mL of DMF under Ar and stirred at 0 °C for 0.5 h. The resultant solution was then exposed to an atmosphere of dry oxygen overnight. The solvent was removed by high-vacuum rotary evaporation, and the green residue was dissolved in 30 mL of $CH_3CN$. This was layered with 100 mL of diethyl ether to precipitate the product, which was then recrystallized from $CH_3CN$/ether (40/120) to give 0.35 g (88%) of air-dried compound. Anal. Calcd for $C_{36}H_{39}N_7Cu_2F_{12}O_4P_2$: C, 41.08; H, 3.84; N, 9.32. Found: C, 41.21; H, 3.97; N, 9.80. Molar conductivity: 131.0 $\Omega^{-1}$ cm$^2$ mol$^{-1}$. EPR ($CHCl_3$/DMF (1:1), 77 K): "silent".

**Oxygenation of 1f-$(PF_6)_2$ using $^{18}O_2$.** Complex **1f-$(PF_6)_2$** (0.21 g, 0.18 mmol) was dissolved in DMF (50 mL) under argon. The solution was then exposed to $^{18}O_2$ for 18 h, while stirring at 0 °C. Solvent was evaporated under reduced pressure, leaving a green residue. Approximately 0.05 g of the greenish residue was dissolved in 3 mL of $CH_3CN$ and recrystallized from 25 mL of $Et_2O$. MS (green solid) (*m*/*z*): 906 ($\{[Cu^{II}_2(NO_2–XYL–O^-)(OH)](PF_6)\}^+$, no $^{18}O_2$ incorporation, but two atoms of $^{16}O$ were found (see Discussion)). The remainder of the green residue was dissolved in 50 mL of $CH_2Cl_2$ and extracted with 30 mL of $NH_4OH$. Reducing the volume of $CH_2Cl_2$ resulted in the isolation of crude oil, which was chromatographed with 100% methanol on silica gel ($R_f$ = 0.43). A total 0.08 g of pure product ($NO_2$–XYL–OH) was recorded for a yield of 73%. MS (*m*/*z*): 618 ($MH^+$, ($NO_2$–XYL–OH), no $^{18}O_2$ incorporation, but indicates incorporation of one $^{16}O$ atom into this phenol (see Discussion)).

**Oxygenation of 1b-$(PF_6)_2$ in $CH_2Cl_2$ at Low Temperature. Isolation of $[Cu^{II}_2(MeO–XYL–H(OH))](PF_6)_3$ (5b-$(PF_6)_3$).** Compound **1b-$(PF_6)_2$** (0.5 g, 0.48 mmol) was dissolved in 50 mL of $CH_2Cl_2$ under Ar, and after the temperature was lowered to −80 °C, the solution was exposed to an atmosphere of dry oxygen for 0.5 h. The color of the solution did not change, but increasing the temperature to ~ −30 °C caused the color to change to greenish, which then changed to dark green with further warming. Near 0 °C the color changed to purple brown along with some green precipitate. The mixture was filtered, and the green precipitate was recrystallized from $CH_3CN$/ether to give ~0.18 g (16%) of pure unhydroxylated compound formulated as $[Cu^{II}_2(MeO–XYL–H(OH))](PF_6)_3$. Anal. Calcd for $Cu_2C_{37}H_{43}N_6O_2P_3F_{18}$: C, 38.11; H, 3.69; N, 7.21. Found: C, 37.76; H, 3.59; N, 7.21. IR (Nujol; $cm^{-1}$): 3630 (OH), 840 ($PF_6$). UV–visible ($CH_3CN$) $\lambda_{max}$, nm ($\epsilon$, $M^{-1}\ cm^{-1}$)): 253 (sh, 17 100), 290 (sh, 5560), 680 (240). Molar conductivity: 204.0 $\Omega^{-1}\ cm^2\ mol^{-1}$.

**Oxygenation of Compound 1c-$(PF_6)_2$ in $CH_2Cl_2$ at Low Temperature. Isolation of $[Cu^{II}_2$(*t*-Bu–XYL–H(OH))]$(PF_6)_3 \cdot 4H_2O$ (5c-$(PF_6)_3$).** Complex **1c-$(PF_6)_2$** was prepared *in situ* by mixing *t*-Bu–XYL (0.3 g, 0.49 mmol) and $[Cu^I(CH_3CN)_4]PF_6$ (0.365 g, 0.98 mmol) in 40 mL of $CH_2Cl_2$ while stirring under argon. After 20 min, the temperature was lowered to –80 °C and the yellow solution was exposed to an atmosphere of dry dioxygen for 2 h. The solution began to turn dark-green. The mixture was slowly warmed to room temperature, whereupon a blue precipitate developed along with a green filtrate. The mixture was filtered, and the blue precipitate was then recrystallized from $CH_3CN$ (30 mL) and ether (150 mL), while standing for 3 days at 0 °C. The resulting blue powder was washed with 30 mL of ether and air-dried (0.10 g, 16%). Anal. Calcd for $C_{40}H_{57}N_6Cu_2F_{18}O_5P_3$: C, 38.01; H, 4.51; N, 6.65. Found: C, 37.73; H, 4.09; N, 6.73. IR (Nujol; $cm^{-1}$): 3450 (m, br, $H_2O$), ca. 2900 (s, C—H), 1610 (C=C), ca. 840 (s, br, $PF_6$). UV–visible ($CH_3CN$) $\lambda_{max}$, mm ($\epsilon$, $M^{-1}\ cm^{-1}$) 263 (22 300), 290 (sh, 8500), 694 (200). Molar conductivity: 198.0 $\Omega^{-1}\ cm^2\ mol^{-1}$. EPR ($CHCl_3$/DMF (1:1), 77 K): "silent". MS (*m/z*): 957 $[Cu^{II}_2$(*t*-Bu–XYL)$(PF_6)_{1.5}]$, 675 $[Cu^{II}$(*t*-Bu–XYL)$]^{2+}$, 612 (*t*-Bu–XYL). Ligand analysis, TLC in 100% EtOAc on alumina: *t*-Bu–XYL $R_f = 0.32$; blue solid $R_f = 0.32$.

**Oxygenation of Compound 1f-$(PF_6)_2$ in $CH_2Cl_2$ at Low Temperature. Isolation of $[Cu^{II}_2(NO_2–XYL–H(OH))](PF_6)_3 \cdot H_2O$ (5f-$(PF_6)_3$).** This reaction was done similarly to the oxygenation of complex **1c** by mixing $NO_2$–XYL (0.3 g, 0.52 mmol) and $[Cu^I(CH_3CN)_4](PF_6)$ (0.38 g, 1.03 mmol) in 35 mL of $CH_2Cl_2$ and oxygenating at –80 °C for 3 h, whereupon initially a purple color was formed. After some time, the purple color disappeared and some precipitate formed along with a green solution. After 3 h the precipitate was filtered, and the clear filtrate was discarded. The precipitate was washed with 20 mL of $Et_2O$ and air-dried to give 0.60 g of a greenish colored powder. This powder was then dissolved in 40 mL of $CH_3CN$ and precipitated with 200 mL of $Et_2O$. The crude powder at this stage consisted of two solid products, which could be purified by fractional crystallization. After this powder was dissolved in 25 mL of $CH_3CN$, a blue solid developed within 24 h with a clear, green filtrate. This was filtered, and the blue solid was then recrystallized from $CH_3CN$ (40 mL) and $Et_2O$ (150 mL) to give 0.15 g (24%) of pure material. Anal. Calcd for $C_{36}H_{42}N_7Cu_2F_{18}O_4P_3$: C, 36.05; H, 3.53; N, 8.17. Found: C, 35.89; H, 3.77; N, 8.14. IR (Nujol; $cm^{-1}$): 3450 (m, br, $H_2O$) ca. 2900 (s, C—H), 1610 (s, br, C=C), 1580 (w, $NO_2$ asymmetric), 1450 (s), 1380 (s, $NO_2$ symmetric), ca. 840 (s, br, $PF_6$), UV–visible ($CH_3CN$) $\lambda_{max}$, nm ($\epsilon$, $M^{-1}\ cm^{-1}$) 261 (28 840), 688 (230). Molar conductivity: 195.0 $\Omega^{-1}\ cm^2\ mol^{-1}$. EPR ($CHCl_3$/DMF (1:1), 77 K): "silent". MS (*m/z*): 727 $[Cu^{II}_2(NO_2–XYL)]^{4+}$, 664 $[Cu^{II}(NO_2–XYL)]^{2+}$, 601 $[NO_2–XYL]$. Ligand analysis, TLC in 100% EtOAc on alumina: $NO_2$–XYL $R_f = 0.55$; blue solid $R_f = 0.55$.

**Manometry: $O_2$-Uptake for 1c-$(PF_6)_2$.** The method used for $O_2$-uptake is described elsewhere.[26] The absorption of dioxygen by the complex in DMF was monitored at 0 °C and constant pressure. For two runs using ca. 0.5 mmol of complex **1c-$(PF_6)_2$**, the $Cu/O_2$ ratio was found to be $2Cu/0.96O_2$.

**$O_2$-Uptake for 1f-$(PF_6)_2$.** The absorption of dioxygen by the complex in DMF was monitored at 0 °C and constant pressure, similar to the case of complex **1c-$(PF_6)_2$**. For two runs using ca. 0.5 mmol of complex **1f-$(PF_6)_2$**, the $Cu/O_2$ ratio was found to be $2Cu/0.95O_2$.

**Stopped-Flow Kinetics Studies.**

**A. Solutions.** Dioxygen-sensitive solutions of compounds **1a–f** were prepared and handled using techniques analogous to those previously described,[29a] however, using $CH_2Cl_2$ instead of propionitrile as the solvent. These solutions were mixed with dioxygen or air-saturated $CH_2Cl_2$. The solubility of $O_2$ was determined manometrically, from the dioxygen uptake of degassed $CH_2Cl_2$ at 298 K and 720 Torr; the value observed was 0.0038 mol/L. Concentrations of solutions at various temperatures were calculated from those determined at room temperature, taking into account the thermal expansion of $CH_2Cl_2$.

**B. Instrumentation, Software, and Data Reduction.** All kinetics experiments were performed using a modified SFL-21 low-temperature flow unit (Hi-Tech Scientific) and data collection device as described in detail previously.[29a] Each experiment consisted of 50 complete spectra (508 diode readings between 359 and 760 nm). Factor analysis was used throughout for primary compression of the data sets. Calculation of the individual rate constants was done by numerical integration of the appropriate rate laws as also described in ref 29a. As an alternative, two exponentials could in many cases be fitted to the data and subsequently converted into the correct model containing, e.g., $k_1$, $k_{-1}$, and $k_2$, by a method previously described by Rodiguin.[48] The latter method in general was faster and simpler for experiments which were done under pseudo-first-order conditions, i.e., in the presence of a large excess of $O_2$.

**C. Kinetics Experiments.** For the individual complexes, 75 (**1c**) to 200 (**1a**) complete experiments were run. Concentrations were varied between $8.0 \times 10^{-5}$ M (**1c**) and $7.1 \times 10^{-4}$ M (**1d**), and temperatures ranged from 178 to 298 K for **1a**, 171 to 299 K for **1c**, 188 to 248 K for **1d**, and 180 to 262 K for **1f**. A considerable number of the runs were not included into the set of data used for the final calculation of the activation parameters, be it for excessive photochemical interference,[5] for lack of significant spectral changes at the highest temperatures, or since the experiments were simply used to check reproducibility. The number of runs taken as final data sets were 66 (**1a**), 25 (**1c**), 91 (**1d**), and 45 (**1f**). Data collection times ranged from 0.4 to 200 s for **1a**, 2 to 60 s for **1c**, 3 to 300 s for **1d**, and 10 to 180 s for **1f**. Experimental conditions for the methoxy and cyano derivatives **1b** and **1e** were in the same range but are not listed, as no reliable parameters could be obtained for these two complexes.

**Acknowledgment.** We are grateful to the National Institutes of Health (Grant GM28962, K.D.K.) and the Swiss National Science Foundation (A.D.Z.) for support of this research.

**Supplementary Material Available:** $^1H$ and $^{13}C$ NMR chemical shifts of free ligands and copper complexes (Tables S1 and S2) and Eyring plots for complexes **1c** and **1d** (4 pages). This material is contained in many libraries on microfiche, immediately follows this article in the microfilm version of the journal, and can be ordered from the ACS; see any current masthead page for ordering information.

---

(48) Rodiguin, N. M.; Rodiguina, E. N. *Consecutive Chemical Reactions*; D. van Nostrand Co., Inc.: Princeton, NJ, 1964.